Molecular Therapy
Methods & Clinical Development
Original Article

Preclinical Development of an AAV8-hUGT1A1 Vector for the Treatment of Crigler-Najjar Syndrome

Fanny Collaud,[1,6] Giulia Bortolussi,[2,6] Laurence Guianvarc'h,[1,6] Sem J. Aronson,[3] Thierry Bordet,[4] Philippe Veron,[1] Severine Charles,[1] Patrice Vidal,[1] Marcelo Simon Sola,[1] Stephanie Rundwasser,[1] Delphine G. Dufour,[1] Florence Lacoste,[1] Cyril Luc,[1] Laetitia v. Wittenberghe,[1] Samia Martin,[1] Christine Le Bec,[1] Piter J. Bosma,[3] Andres F. Muro,[2] Giuseppe Ronzitti,[1] Matthias Hebben,[1] and Federico Mingozzi[1,5]

[1]INTEGRARE, Genethon, INSERM, Univ. Evry, Université Paris-Saclay, 91002 Evry, France; [2]International Center for Genetic Engineering and Biotechnology, 34149 Trieste, Italy; [3]Amsterdam UMC, University of Amsterdam, Tytgat Institute for Liver and Intestinal Research, AG&M, 1105 BK Amsterdam, the Netherlands; [4]AFM-Telethon, 91000 Evry, France

Adeno-associated viruses (AAVs) are among the most efficient vectors for liver gene therapy. Results obtained in the first hemophilia clinical trials demonstrated the long-term efficacy of this approach in humans, showing efficient targeting of hepatocytes with both self-complementary (sc) and single-stranded (ss) AAV vectors. However, to support clinical development of AAV-based gene therapies, efficient and scalable production processes are needed. In an effort to translate to the clinic an approach of AAV-mediated liver gene transfer to treat Crigler-Najjar (CN) syndrome, we developed an (ss)AAV8 vector carrying the human UDP-glucuronosyltransferase family 1-member A1 (hUGT1A1) transgene under the control of a liver-specific promoter. We compared our construct with similar (sc)AAV8 vectors expressing hUGT1A1, showing comparable potency *in vitro* and *in vivo*. Conversely, (ss)AAV8-hUGT1A1 vectors showed superior yields and product homogeneity compared with their (sc) counterpart. We then focused our efforts in the scale-up of a manufacturing process of the clinical product (ss)AAV8-hUGT1A1 based on the triple transfection of HEK293 cells grown in suspension. Large-scale production of this vector had characteristics identical to those of small-scale vectors produced in adherent cells. Preclinical studies in animal models of the disease and a good laboratory practice (GLP) toxicology-biodistribution study were also conducted using large-scale preparations of vectors. These studies demonstrated long-term safety and efficacy of gene transfer with (ss)AAV8-hUGT1A1 in relevant animal models of the disease, thus supporting the clinical translation of this gene therapy approach for the treatment of CN syndrome.

INTRODUCTION

Crigler-Najjar (CN) syndrome is a rare and severe condition that affects bilirubin metabolism.[1,2] The disease is due to mutations in the liver-specific enzyme UDP-glucuronosyltransferase family 1-member A1 (UGT1A1) that conjugates bilirubin and mediates its disposal. The lack of this enzyme results in the accumulation of unconjugated bilirubin in serum, which is associated with brain toxicity and early death.[3] CN syndrome is an inherited autosomal recessive disorder with an incidence of about 1 in 1,000,000 newborns. Therapy for CN syndrome consists of daily cycles of 12–16 h of exposure to blue light, which results in bilirubin photoisomerization and elimination in the urine. However, poor compliance to phototherapy and loss of efficacy associated with aging expose patients to potentially lethal bilirubin spikes.[3,4] At present, there is no authorized medicinal product for the treatment of CN syndrome, and orthotopic liver transplantation is the only curative treatment, with all the limitations of the approach.[3–6]

The monogenic etiology of the disease, the absence of liver parenchymal damage, and the low levels of UGT1A1 enzyme activity needed to correct the phenotype[7] make CN syndrome an ideal target for gene therapy.[8,9] Adeno-associated virus (AAV) vector-mediated gene therapy is one of the most promising approaches for safe and efficient gene transfer to the liver.[10] The efficacy of liver-directed AAV gene therapy is demonstrated by the recent successes in patients with hemophilia A and B[11–15] and by the growing number of clinical trials using AAV vectors to transfer therapeutic transgenes to the liver.

Several studies showed therapeutic efficacy following AAV vector-mediated gene transfer to the liver in both mouse and rat models of CN syndrome.[16–20] Accordingly, we recently showed long-term correction of bilirubin levels following liver-directed gene transfer

Received 9 October 2018; accepted 26 December 2018;
https://doi.org/10.1016/j.omtm.2018.12.011.

[5]CureCN consortium

[6]These authors contributed equally to this work.

Correspondence: Federico Mingozzi, PhD, INTEGRARE, Genethon, INSERM, Univ. Evry, Université Paris-Saclay, 1 rue de l'Internationale, 91002 Evry, France.
E-mail: fmingozzi@genethon.fr

This is an open access article under the CC BY-NC-ND license (http://creativecommons.org/licenses/by-nc-nd/4.0/).

Genzyme Ex. 2020
Sarepta Therapeutics, Inc. v. Genzyme Corporation
Page 1 of 18

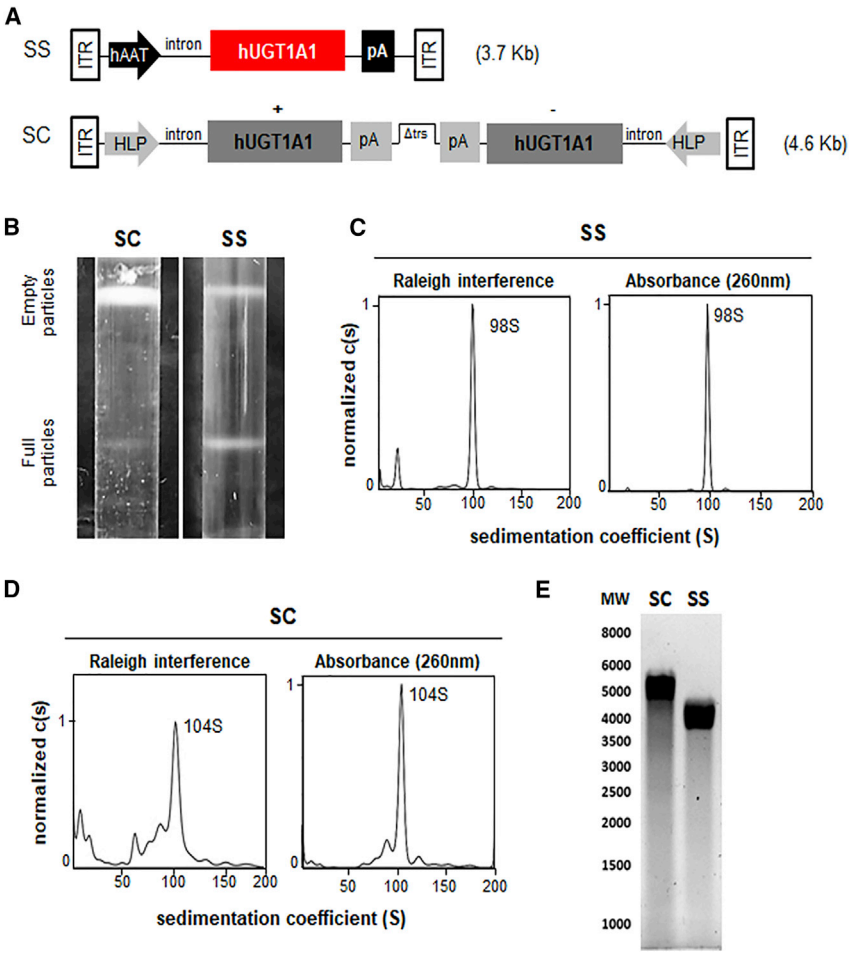

Figure 1. (sc)AAV8-hUGT1A1 and (ss)AAV8-hUGT1A1 Vector Comparison

(A) Schematic representation of the transgene expression cassettes. (ss)AAV8-hUGT1A1 (SS) and (sc)AAV8-hUGT1A1 (SC) cassettes are composed of a liver-specific promoter, an intron, a poly-A (pA), and the sequence of human UGT1A1 (hUGT1A1). The SC expression cassette contains a truncated ITR (Δtrs) that allows for self-complementary genome packaging. (B) Purification profiles of (ss)AAV8-hUGT1A1 (SS) and (sc)AAV8-hUGT1A1 (SC) vectors after ultracentrifugation in cesium chloride gradient. The higher bands contain empty particles and the lower bands contain full particles. (C and D) Sedimentation profiles of (ss)AAV8-hUGT1A1 (C) and (sc)AAV8-hUGT1A1 (D) full particles purified by cesium chloride gradient and subjected to analytical ultracentrifugation. In each graph, the x axis represents the sedimentation coefficient expressed in Svedberg units (S), and the y axis represents the normalized value of the concentration as a function of S (c(S)), measured by Raleigh interference or absorbance at 260 nm. (E) Denaturing gel performed on genomic extracts obtained from (sc)AAV8-hUGT1A1 (SC) or (ss)AAV8-hUGT1A1 (SS). Molecular weight (MW) is indicated on the left.

with an AAV8 vector expressing a codon-optimized version of the UGT1A1 cDNA.[19]

However, one of the biggest challenges for the clinical translation of AAV vector-based therapies is vector production. In particular, scalable production systems able to deliver high-yield and high-purity material are needed.[21] Several AAV vector production platforms have been used to produce clinical-grade vector lots, although in recent years the field coalesced around transfection- and baculovirus-based production methods.[22]

Here, in an effort to develop and translate to the clinic a gene therapy for CN syndrome, we developed an AAV8 vector to efficiently express the human UGT1A1 (hUGT1A1) transgene in hepatocytes. We initially compared single-stranded (ss)AAV and self-complementary (sc)AAV vector genome (vg) configurations, showing a nearly identical potency profile *in vitro* and *in vivo*. However, based on the yields in production and the impurities profile, we focused production scale-up and preclinical studies on a (ss)AAV8-hUGT1A1 vector. A bioreactor system for the triple transfection HEK293 cells grown in suspension was established. Dose-finding studies were conducted in two animal models of the CN syndrome using full-scale vector preparations. In parallel, good laboratory practice (GLP) studies were performed to evaluate toxicity, vector shedding, and biodistribution of the clinical vector (ss)AAV8-hUGT1A1 in wild-type (WT) rats. Germline transmission studies were also performed, together with a detailed assessment of immunogenicity of the therapeutic product. These results support the initiation of a phase I/II clinical trial in patients (ClinicalTrials.gov: NCT03466463).

RESULTS

(ss)AAV8-hUGT1A1 Vector Preparations Present Better Yields and Higher Product Homogeneity Compared to (sc)AAV8-hUGT1A1 Vectors

We compared (sc)AAV and (ss)AAV vectors encoding for hUGT1A1 under the transcriptional control of liver-specific promoters (Figure 1A). The two expression cassettes were pseudotyped into AAV serotype 8 to efficiently transduce the liver of animals.[12,23] Research-grade vector preparations were obtained by triple transfection of adherent HEK293 cells grown in roller bottles.[22] Purification by cesium chloride gradient of (ss)AAV8-hUGT1A1 resulted in two well-defined bands, corresponding to empty and full particles. Conversely, the full-particle band obtained for (sc)AAV-hUGT1A1 was less intense and diffused (Figure 1B). This was associated with more than a 3-fold reduction in production yields ($6.0 \pm 1.89 \times 10^4$ vg/cell versus $1.77 \pm 1.37 \times 10^4$ vg/cell for (ss) and (sc) AAV, respectively; data obtained from at least two independent production lots).

Genzyme Ex. 2020
Sarepta Therapeutics, Inc. v. Genzyme Corporation
Page 2 of 18

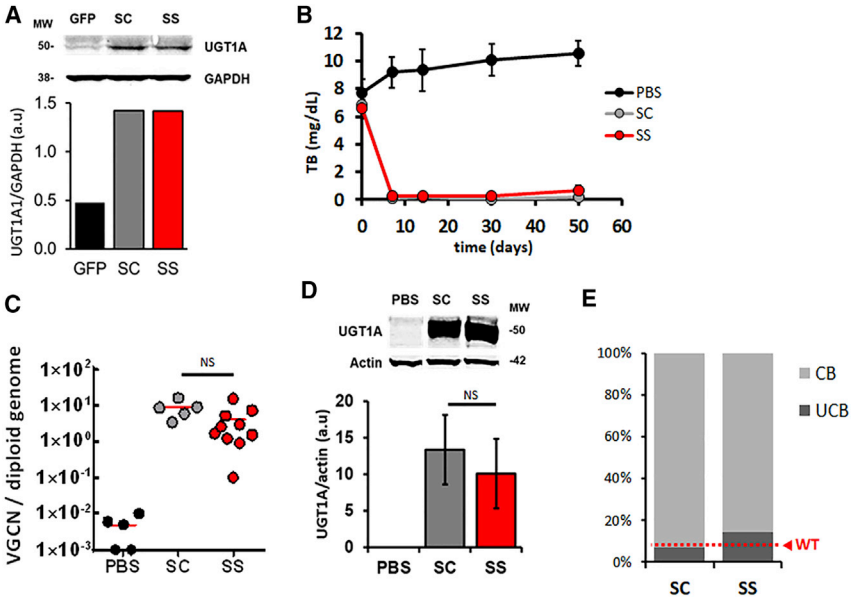

Figure 2. (sc)AAV8-hUGT1A1 and (ss)AAV8-hUGT1A1 Vectors Have Similar Efficacy *In Vitro* and *In Vivo*

(A) Huh7 cells were transduced with AAV8-GFP, (sc)AAV8-hUGT1A1, or (ss)AAV8-hUGT1A1 at 25,000 MOI. At 72 h after transduction, microsomal extracts were obtained, separated by SDS-PAGE, and analyzed by western blot with UGT1A- and GAPDH-specific antibodies. Molecular weight (MW) is indicated on the left and quantification of band intensity is reported. (B–D) 6- to 8-week-old Gunn rats were injected with PBS (PBS), 1×10^{12} vg/rat (sc) AAV8-hUGT1A1 (SC), or the same dose of (ss)AAV8-hUGT1A1 (SS). (B) Total bilirubin (TB) levels measured in serum at the indicated time points. (C) Vector genome copy number (VGCN) per cell measured by qPCR in liver. The graph shows the single values (dots) and the average values (red line) measured in each group and normalized for the number of copies of titin per sample. Statistical analysis was performed by ANOVA (NS, non-significant; PBS n = 5, SC n = 5, SS n = 10). (D) Western blot analysis performed on microsomal extracts from rat livers with UGT1A and actin-specific antibodies. Molecular weight (MW) is indicated on the left and quantification of band intensity is reported. (E) Bilirubin conjugates measured by HPLC in the bile of 8-week-old Gunn rats injected with 5×10^{11} vg/kg (sc)AAV8-hUGT1A1 (SC, n = 6) or (ss)AAV8-hUGT1A1 (SS, n = 10). At 12 weeks after injection, animals were sacrificed and bile was analyzed. The graph shows the percentage of conjugated bilirubin (CB) and unconjugated bilirubin (UCB) measured in bile. The level of unconjugated bilirubin observed in wild-type Wistar rats is reported in red (WT).

We then evaluated the analytical ultracentrifugation (AUC) profile of the full particles obtained for the two vectors. AUC performed on purified (ss)AAV8-UGT1A1 vectors revealed a sharp single peak, with a sedimentation coefficient consistent with the size of the (ss)genome (Figure 1C). Conversely, for (sc)AAV8-hUGT1A1 vectors, we observed the presence of different peaks, possibly due to the presence of AAV vectors containing DNA fragments of variable length (Figure 1D). The integrity of the genome was further analyzed by the separation of purified vgs by electrophoresis under alkaline condition (Figure 1E), confirming the presence of a smear of vgs of different sizes in (sc)AAV8-hUGT1A1 vector preparations. Together, these data indicate that research grade (ss)AAV8-hUGT1A1 vectors were produced with higher yields and were more homogeneous than their (sc) counterpart.

(ss)- and (sc)AAV8-UGT1A1 Vectors Present an Equal Potency Profile *In Vitro* and *In Vivo*

We next compared the transduction efficiency of (sc)AAV8-hUGT1A1 versus (ss)AAV8-hUGT1A1 *in vitro* in human hepatoma cells,[19] which resulted in a similar expression of the hUGT1A1 transgene (Figure 2A). Next, *in vivo* comparison of the vectors was performed in a well-established model of CN syndrome, the Gunn rat.[24–26] This model presents blood levels of bilirubin comparable to those observed in patients with mild symptoms and no evident signs of brain toxicity (6–12 ± mg/dL). (sc)AAV8-hUGT1A1 and (ss)AAV8-hUGT1A1 vectors titered side by side were injected intravenously into 8-week-old Gunn rats (n = 10/group). Total bilirubin (TB) was measured in blood for about 7 weeks post-injection. Systemic injection of 1×10^{12} vg/rat (corresponding to 5.0×10^{12} vg/kg) of both vectors resulted in a complete and sustained normalization of circulating bilirubin levels (Figure 2B). vg copy number (VGCN) analysis and hUGT1A1 protein expression levels in liver measured in treated animals confirmed the equivalence in potency of the two vectors (Figures 2C and 2D). A similar potency of (ss)- versus (sc)AAV8-hUGT1A1 vectors was also observed at 1×10^{10} and 1×10^{11} vg/rat (data not shown).

In a separate experiment, Gunn rats were injected with 5×10^{11} vg/kg of (ss)AAV8-hUGT1A1 or (sc)AAV8-hUGT1A1. At 3 months after vector injection, bilirubin-glucuronide conjugates were present at similar levels in the bile of rats treated with the two vectors (Figure 2E). These data suggest that (ss)- and (sc)AAV8-hUGT1A1 vectors used in the current study transduce hepatocytes equally both *in vitro* and *in vivo*. Based on the comparable efficacy of the two vectors and the higher production yields and homogeneity profile, the (ss)AAV8-hUGT1A1 vector was selected as the lead candidate for clinical development.

(ss)AAV8-hUGT1A1 Can Be Efficiently Produced in HEK293 Cells Grown in Suspension

A fully scalable method based on triple transfection of HEK293 cells cultured in suspension was developed to support the clinical development of (ss)AAV8-hUGT1A1 (Figure S1). Triple transfection of HEK293 cells was performed with polyethylenimine (PEI) directly in 10-l bioreactors. AAV vectors were recovered from both supernatant and cells by mild detergent lysis followed by AVB Sepharose affinity column purification. Purified vectors were then concentrated and tested for quality and potency. AUC performed

Genzyme Ex. 2020
Sarepta Therapeutics, Inc. v. Genzyme Corporation
Page 3 of 18

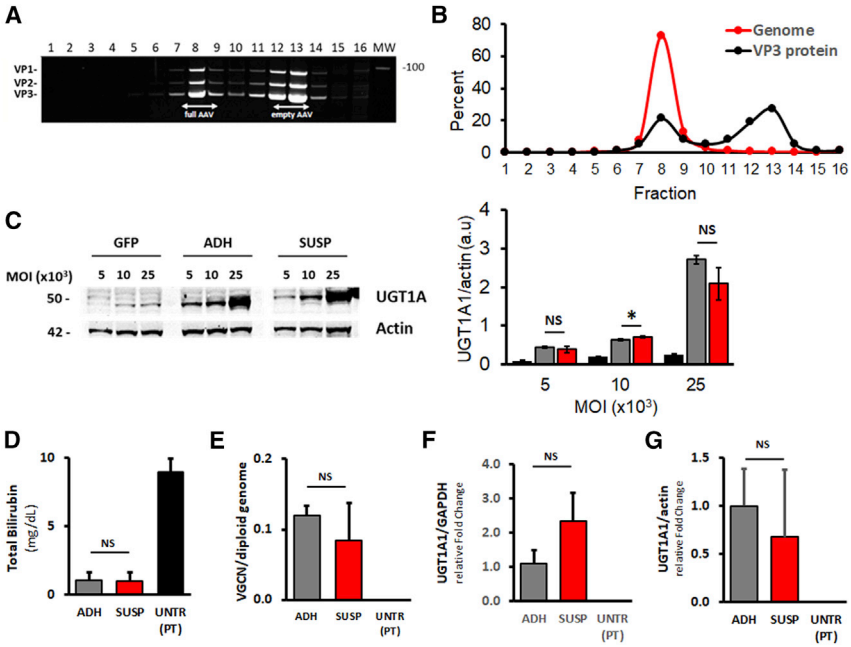

Figure 3. *In Vitro* and *In Vivo* Comparison of (ss)AAV8-hUGT1A1 Produced in HEK293 Cells Growing in Suspension or Adherent

(A and B) Characterization of AAV8 vector expressing hUGT1A1 produced by triple transfection of HEK293 cells cultured in suspension in a medium-scale bioreactor (10 L) and purified by affinity chromatography (SUSP). (A) Suspension-produced vector was loaded in a cesium chloride gradient ultracentrifugated and fractionated in 16 fractions starting from the bottom of the tube. Each fraction was analyzed by SDS-PAGE (lanes 1–16) and stained with SYPRO Ruby. Molecular weight is indicated on the right. (B) VP3 intensity of each fraction was quantified and the percentage of each fraction was plotted in the graph (VP3 protein). Genome titer was measured in each fraction by qPCR. The percentage was calculated as the number of copies in each fraction divided by the sum of the copies in the whole fractions (Genome). (C) Huh7 cells were transduced with AAV8-GFP (GFP), (ss)AAV8-hUGT1A1 produced in HEK293 cells cultured in adhesion (ADH), or in suspension (SUSP) at 5,000, 10,000, and 25,000 MOI. At 72 h post-transduction, microsomal extracts were obtained, separated by SDS-PAGE, and analyzed by western blot with UGT1A and actin antibodies. Molecular weight is indicated on the left. Quantification of band intensity is reported on the right. (D–G) *In vivo* comparison in a mouse model of hyperbilirubinemia. Ugt1a1$^{-/-}$ mice were injected with vehicle (PBS) or 3.3 × 10^{9} vg/mouse (ss)AAV8-hUGT1A1 vectors produced in HEK293 cells in adhesion (ADH) or in suspension (SUSP). (D) TB levels were analyzed 30 days after vector injection. (E) Vector genome copy number (VGCN) analysis, (F) normalized hUGT1A1 mRNA levels, and (G) protein expression by western blot in livers of Ugt1a1$^{-/-}$ mice analyzed 30 days post-treatment are shown. Data are reported as mean ± SD. Statistical analyses were performed by ANOVA (*$p < 0.05$; NS, non-significant; UNTR (PT) n = 4, ADH n = 4, SUSP n = 3).

on (ss)AAV8-hUGT1A1 vector produced in suspension revealed that the product contained around 20% of full capsids (data not shown). To better characterize the full-to-empty particles ratio, the purified (ss)AAV8-hUGT1A1 final product was loaded on a cesium chloride gradient, and 16 fractions were collected and analyzed for capsid protein and DNA content. SDS-PAGE followed by Sypro Ruby staining revealed the presence of the three bands corresponding to viral protein (VP)1, VP2, and VP3 at a ratio of 1:1:10 (Figure 3A). Two populations of particles, peaking at fractions 8 and 12–13, were identified. Subsequent qPCR analysis showed that fractions 8 and 12–13 corresponded to full and empty particles, respectively (Figure 3B). Consistent with the AUC analysis, AAV particles present in fraction 8 represented 21% of the total VP protein, and qPCR data indicated that this fraction contained full capsids, representing 72.9% of AAV genomes present in all fractions.

We then evaluated the *in vitro* potency of the vector produced in suspension. Huh-7 cells were transduced with increasing MOIs of (ss) AAV8-hUGT1A1 produced in adherent cells or in suspension at 10-L scale. Similar levels of hUGT1A1 protein were detectable by western blot in cell lysates obtained from cells transduced with the two vector preparations (Figure 3C).

The equivalence of the two vectors was further confirmed *in vivo* in a juvenile Ugt1 knockout mouse model (Ugt1$^{-/-}$).[16,17] These mice present a phenotype that closely resembles the human condition; therefore, they need to be exposed to phototherapy (PT) to survive. 11-day-old mice were injected with 3.3 × 10^{9} vg/mouse (corresponding to 5.0 × 10^{11} vg/kg) of (ss)AAV8-hUGT1A1 vector produced in adherent or in suspension HEK293 cells. At 1-month post-injection, plasma bilirubin levels were determined, and a complete correction of total serum bilirubin levels (about 1.0 mg/dL) was observed in mice treated with both AAV vector preparations (Figure 3D). VGCN analysis demonstrated that the two vectors transduced hepatocytes with similar efficacy (Figure 3E). Accordingly, the expression of hUGT1A1 mRNA and protein levels in the livers of AAV vector-treated Ugt1$^{-/-}$ mice analyzed 30 days post-treatment was comparable (Figures 3F and 3G). These results demonstrate that the potency of vectors produced in bioreactors are fully comparable with research-grade vectors derived from adherent cells.

Dose-Finding Studies with Large-Scale Preparation of (ss)AAV8-hUGT1A1

We next scaled up the 10-l suspension AAV production to 200 L. Several 200-L lots of (ss)AAV8-hUGT1A1 vectors were produced, demonstrating robustness and reproducibility of the process. AUC analysis revealed that the large-scale product contained >30% of full capsids (Figure 4A). The vector potency was then evaluated *in vitro*. Treatment of Huh-7 cells at a 25,000 MOI of (ss)AAV8-hUGT1A1 resulted in hUGT1A1 protein levels similar to those obtained with adherent cells and medium scale (Figure S2).

Next, a dose escalation study was conducted in Gunn rats, starting at vector doses that have previously shown therapeutic efficacy.[19] At

Genzyme Ex. 2020
Sarepta Therapeutics, Inc. v. Genzyme Corporation
Page 4 of 18

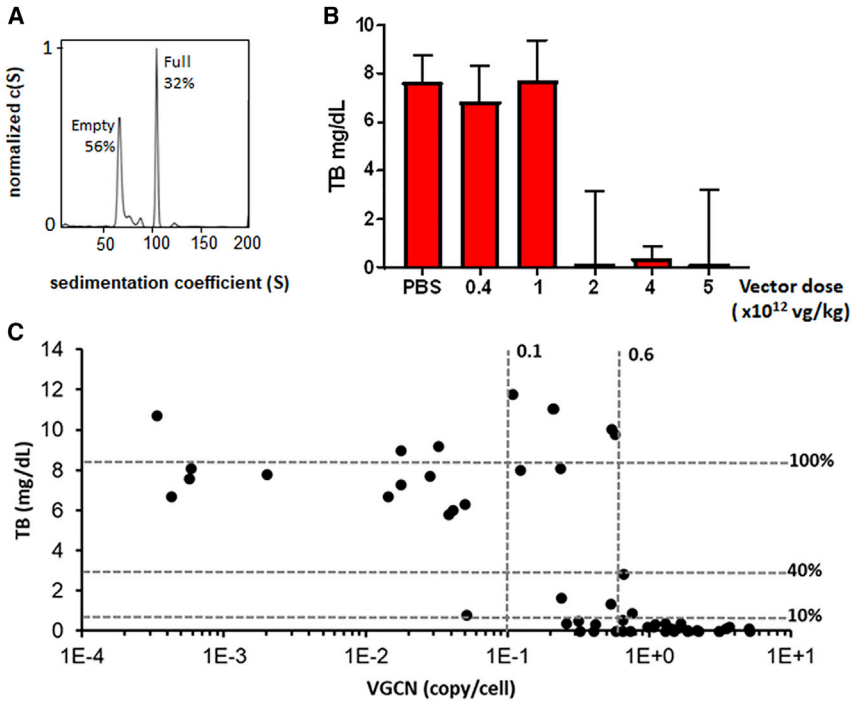

Figure 4. Non-GLP Dose-Finding Study with Large-Scale-Produced (ss)AAV8-hUGT1A1 Vector

(A) Sedimentation profile obtained by analytical ultracentrifugation of (ss)AAV8-hUGT1A1 vector, produced by triple transfection of HEK293 cells in suspension at large scale (150 L) and purified by affinity chromatography. The x axis represents the sedimentation coefficient expressed in Svedberg units (S), and the y axis represents the normalized value of the concentration as a function of S (c(S)) measured by Raleigh interference. (B and C) 8-week-old Gunn rats were injected intravenously with PBS (PBS) or (ss)AAV8-hUGT1A1 at the indicated doses. Total bilirubin (TB) levels in plasma and vector copy number (VGCN) in liver were assessed 84 days post-injection. (B) Median with range of TB levels in plasma are shown. (C) TB levels are plotted against VGCN in liver. Data from all animals are shown.

2 weeks after systemic injection of 6- to 8-week-old rats, blood samples were collected, and TB was analyzed. A dose-dependent decrease in the levels of plasma TB was seen in animals treated with the (ss) AAV8-hUGT1A1 (Figure 4B). At a dose of 1×10^{12} vg/kg, 4/11 rats showed a correction of TB levels, while, at 2×10^{12} vg/kg, in 8/10 rats a full correction of hyperbilirubinemia was observed (Figure 4B; data not shown). vg copies determined in whole livers of treated Gunn rats 84 days after treatment also showed a dose-dependent increase and correlated with the levels of correction of TB in serum. (Figure 4C). Based on these results, VGCN below 0.1 copies/cell was not sufficient to correct TB levels, as 13/14 animals with VGCN < 0.1 copies/cell had TB levels >5 mg/dL. VGCN per cell in the range of 0.1 to 0.6 mediated TB correction in 6/14 rats, while all animals with VGCN per cell greater than 0.6 had normal TB levels.

Dose-finding studies were also performed in $Ugt1^{-/-}$ mice. Adult (60- to 90-day-old) male and female $Ugt1^{-/-}$ mice were injected with different doses of (ss)AAV8-hUGT1A1 (from 1.0×10^{11} to 5.0×10^{12} vg/kg) (Figure 5). Plasma bilirubin levels were monitored for 9 months post-injection. Male mice showed bilirubin levels below 0.5 mg/dL at all the doses tested, starting at 1×10^{11} vg/kg (Figure 5A). In female animals, in contrast, after the initial drop of TB levels to WT levels 1 month post-injection (Figure 5B), some animals lost expression over time (see Figure S3 for single-animal TB levels). At 9 months post-injection, mice were sacrificed and livers were harvested for molecular analysis. VGCN (VG/cell) in whole livers showed a dose-response course (Figure 5C), and it correlated well with the level of Ugt1a1 protein determined by western blot analysis and immunofluorescence (Figure 5D; Figure S4). Some inconsistencies in vector dose response were noted in female animals, likely due to sex-specific differences in the efficiency of liver transduction in rodents.[27] Histological analysis of livers revealed no obvious abnormalities, as determined by H&E, Masson trichromic, Sirius red, periodic acid-schiff (PAS), and oil red stainings (Figure S5).

We next performed an additional comparison study in mice and rats using an AAV8 expressing human coagulation factor IX (hFIX) under the transcriptional control of a liver-specific promoter. We first ran a pilot study, which demonstrated that the extent of liver transduction of AAV vectors in rats of Wistar and Sprague-Dawley backgrounds is similar (data not shown). Then, we compared hFIX expression levels in Wistar rats (both WT and $Ugt1a1^{-/-}$) with C57BL/6 mice. At a dose of 5×10^{12} vg/kg, mice showed levels of hFIX > 10 μg/mL (Figure 5F), while rats expressed approximately 1.5 μg/mL hFIX. Interestingly, hFIX expression levels in rats were in a similar range, although still higher, of those observed in hemophilia B patients receiving 2×10^{12} vg/kg of a similar vector.[12] The evaluation of the VGCN in the two species supported the findings on hFIX transgene expression levels (Figure 5G). Together, these results indicate that the rat is a good predictive model of the efficacy of liver gene transfer in humans, in particular for AAV8 vectors, and they support further preclinical studies, including toxicology/biodistribution study in this species.

GLP Toxicity, Biodistribution, and Shedding Study to Support the Safety of Liver Gene Transfer with (ss)AAV8-UGT1A1

A GLP toxicology/biodistribution study was performed in WT adult Sprague-Dawley rats. This was based on the observation that Wistar and Sprague-Dawley have similar levels of liver transduction with AAV vectors (data not shown). The aim of this study was to evaluate the potential toxicity and to determine shedding and biodistribution of the vgs after single intravenous

Genzyme Ex. 2020
Sarepta Therapeutics, Inc. v. Genzyme Corporation
Page 5 of 18

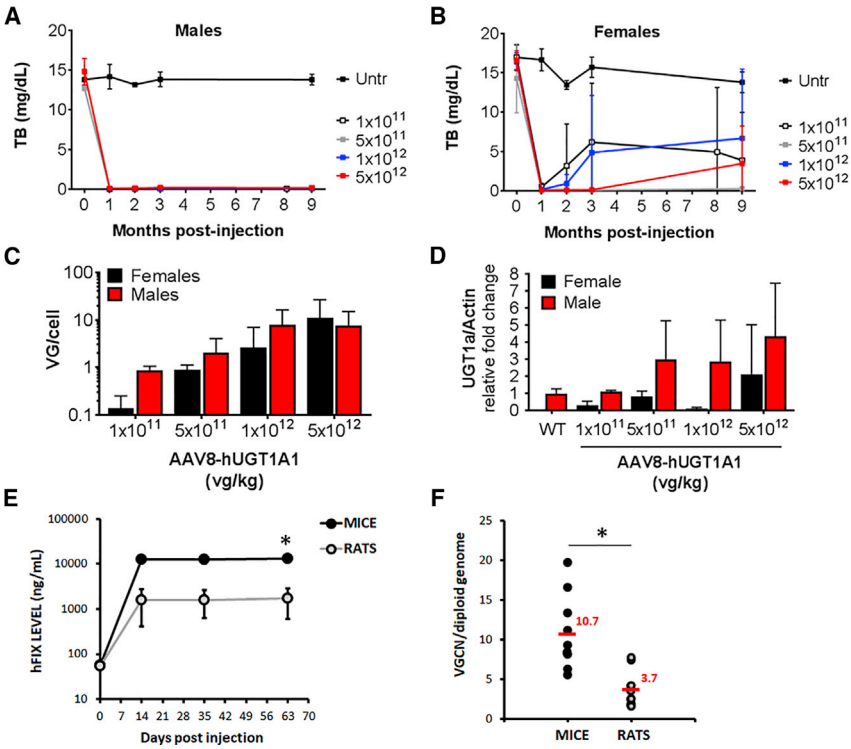

Figure 5. Non-GLP Dose-Finding Study of (ss)AAV8-hUGT1A1 Vector in Adult Ugt1$^{-/-}$ Mice

Ugt1$^{-/-}$ mice were injected as adults with the indicated doses (vg/kg). At 1, 2, and 3 months post-injection, mice were bled and TB levels in plasma were analyzed. At 9 months post-injection, mice were sacrificed and molecular analysis was carried out. (A and B) Plasma bilirubin determination in male (A) and female (B) Ugt1$^{-/-}$ mice. (C) Viral genome copy number (VG/cell) at 9 months post-injection in male and female mice treated with different doses of rAAV8-hUGT1A1. (D) Western blot analysis of liver total protein extracts at 9 months post-injection. 1×10^{11} dose, male n = 5 and female n = 5; 5×10^{11} dose, male n = 3 and female n = 2; 1×10^{12} dose, male n = 8 and female n = 5; 5×10^{12} dose, male n = 6 and female n = 5. (E and F) Wistar rats (WT and UGT1A1-deficient rats; n = 10) and C57BL/6 mice (n = 10) were injected with 5×10^{12} vg/kg of an AAV8 vector expressing human coagulation FIX (hFIX). (E) Levels of circulating hFIX were measured by ELISA and reported in the graph. (F) Liver genome copy number analysis performed 2 months after vector injection. Data are shown as genome copy number per cell normalized on titin gene. Statistical analyses were performed by ANOVA (*$p < 0.05$ as indicated).

administration of (ss)AAV8-hUGT1A1 in WT rats, with a 26-week follow-up. Two vector doses were injected, one equivalent to the maximum planned clinical dose (5×10^{12} vg/kg) and one five times higher (2.5×10^{13} vg/kg).

Overall, the vector was well tolerated with no evident signs of toxicity. There were no unexpected deaths related to the treatment, no adverse in-life findings, no clinical pathology, no changes in biochemical and hematological parameters (Table 1), and no macroscopic findings in animals that received (ss)AAV8-hUGT1A1 and in control animals. Following intravenous administration, the vector was cleared from blood and urine within 29 days, with levels of vgs completely indistinguishable from the limit of quantification (LOQ) of the measurement method (Figures 6A and 6B). At 8 days after vector injection, VGCN and hUGT1A1 mRNA expression levels were measured. No differences in biodistribution were observed between male and female rats. The highest copies of vector were detected in the liver, spleen, and lymph nodes, reflecting the tropism of AAV8 vector following intravenous delivery. hUGT1A1 mRNA was detectable on day 8 in all tissues, at levels at least 2-log lower than those measured in the liver, which was the tissue with the highest copies and the highest mRNA expression, reflecting the specificity of the promoter expressing the hUGT1A1 transgene (Figure 6C; Table S1). Expression of hUGT1A1 in the liver at days 91 and 182 did not show any significant decrease in transgene expression (Figure 6D). Transgene expression was further confirmed by *in situ* hybridization (ISH) in rat liver tissue at day 182 (Figure 6E), showing ~11.5% of hepatocytes expressing the UGT1A1 transgene.

The persistence of vector in gonads at low levels (VGCN < 0.1 per diploid genome) was detected 6 months post-treatment. Based on this, although the risk of germline transmission was expected to be low, we used ISH to further investigate the exact localization of the vector within the gonads. While a signal was localized in ovaries of rats injected with the highest vector dose, positivity was detectable only within the stroma and in blood capillaries. No signal was detected in oocytes (Figure 6F).

A separate GLP study was aimed at assessing the risk of germline transmission in male animals. (ss)AAV8-hUGT1A1 was administered to male rabbits at a dose of 5×10^{12} vg/kg. vgs were determined by qPCR in liver, testis, and epididymis, collected at the day of sacrifice, 150 days after treatment (Figure 6G). Vector shedding in sperm was evaluated pretreatment and at days 3, 7, 15, 30, 60, 90, 120, and 150 post-treatment. Genomes were quantifiable from day 3 to day 30 and became completely undetectable thereafter (Figure 6H).

These results indicate that the single intravenous injection of (ss)AAV8-hUGT1A1 vector was well tolerated at doses up to 2.5×10^{13} vg/kg. They also indicate that the risk for germline transmission at the doses tested is likely to be very low.

In Mice and Rats, (ss)AAV8-hUGT1A1 Drives the Development of Humoral Responses Directed to the Human Transgene

Humoral immune responses against AAV8 and hUGT1A1 were measured in the context of the GLP toxicology study in rats. All animals developed a significant humoral immune response against the

Genzyme Ex. 2020
Sarepta Therapeutics, Inc. v. Genzyme Corporation
Page 6 of 18

Table 1. GLP Toxicology Study: Biochemistry and Hematology Data

	Males						Females					
	Day 8			Day 91			Day 8			Day 91		
Assay	Vehicle	1×	5×	Vehicle	1×	5×	Vehicle	1×	5×	Vehicle	1×	5×
Biochemistry												
AST (U/L)	90 ± 7	73 ± 12	74 ± 5	85 ± 11	75 ± 8	84 ± 26	78 ± 6	63 ± 5	64 ± 5	70 ± 13	75 ± 9	75 ± 15
ALT (U/L)	78 ± 8	68 ± 14	69 ± 12	59 ± 7	55 ± 7	66 ± 26	53 ± 15	49 ± 9	43 ± 10	53 ± 18	53 ± 13	50 ± 10
ALP (U/L)	280 ± 39	265 ± 43	290 ± 21	103 ± 13	101 ± 15	104 ± 14	190 ± 27	136 ± 32	176 ± 27	61 ± 10	70 ± 16	57 ± 7
GGT (U/L)	2 ± 0	2 ± 0	2 ± 0	2 ± 0	2 ± 0	2 ± 0	2 ± 0	2 ± 0	2 ± 0	2 ± 0	2 ± 0	2 ± 0
CK (U/L)	229 ± 26	238 ± 22	224 ± 36	199 ± 117	136 ± 20	176 ± 63	159 ± 14	193 ± 65	225 ± 20	109 ± 18	129 ± 43	165 ± 75
TBIL (μmol/L)	1.3 ± 0.0	1.3 ± 0.0	1.3 ± 0.0	1.3 ± 0.0	1.3 ± 0.0	1.3 ± 0.0	1.3 ± 0.0	1.3 ± 0.0	1.3 ± 0.0	1.3 ± 0.0	1.3 ± 0.0	1.3 ± 0.0
UREA (mmol/L)	5.1 ± 0.6	4.3 ± 0.1	4.0 ± 0.3	5.4 ± 0.8	5.2 ± 0.6	4.8 ± 0.4	4.4 ± 0.3	4.6 ± 0.3	3.8 ± 0.5	5.1 ± 0.8	5.0 ± 0.8	5.2 ± 0.3
CREAT (μmol/L)	23 ± 1	21 ± 2	16 ± 6	31 ± 4	30 ± 2	29 ± 3	24 ± 2	23 ± 3	26 ± 5	35 ± 4	36 ± 2	35 ± 3
GLUC (mmol/L)	8.58 ± 1.17	18.81 ± 2.91	11.82 ± 2.33	9.65 ± 1.56	9.45 ± 1.91	9.80 ± 2.14	8.67 ± 0.48	10.32 ± 1.14	10.71 ± 1.17	9.18 ± 0.78	9.34 ± 0.85	9.54 ± 1.52
CHOL (mmol/L)	2.2 ± 0.4	2.1 ± 0.9	2.1 ± 0.3	1.5 ± 0.2	1.6 ± 0.3	1.7 ± 0.4	1.9 ± 0.3	2.0 ± 0.6	1.8 ± 0.3	1.8 ± 0.4	1.9 ± 0.4	1.7 ± 0.4
TRIG (mmol/L)	1.19 ± 0.35	1.01 ± 0.38	1.43 ± 0.42	1.18 ± 0.51	1.25 ± 0.38	1.44 ± 0.49	0.44 ± 0.13	0.86 ± 0.44	0.61 ± 0.23	0.83 ± 0.27	0.94 ± 0.43	0.77 ± 0.21
TPROT (g/L)	54 ± 2	54 ± 2	54 ± 1	59 ± 2	60 ± 2	62 ± 1	57 ± 2	57 ± 2	56 ± 3	65 ± 3	68 ± 4	67 ± 4
ALB (g/L)	41 ± 2	40 ± 3	40 ± 1	41 ± 2	42 ± 1	41 ± 2	45 ± 2	43 ± 2	42 ± 3	50 ± 3	52 ± 3	51 ± 3
GLOB (g/L)	13 ± 1	14 ± 3	13 ± 1	18 ± 2	19 ± 1	21 ± 2	13 ± 1	14 ± 2	13 ± 1	15 ± 2	16 ± 2	16 ± 2
A/G	3.1 ± 0.5	2.9 ± 0.8	3.0 ± 0.2	2.3 ± 0.3	2.2 ± 20.1	2.0 ± 0.2	3.6 ± 0.3	3.3 ± 0.5	3.2 ± 0.3	3.5 ± 0.6	3.4 ± 0.6	3.2 ± 0.4
CA (mmol/L)	2.77 ± 0.08	2.76 ± 0.04	2.74 ± 0.07	2.52 ± 0.11	2.55 ± 0.08	2.60 ± 0.06	2.72 ± 0.07	2.69 ± 0.09	2.68 ± 0.07	2.61 ± 0.08	2.64 ± 0.11	2.62 ± 0.13
PHOS (mmol/L)	2.14 ± 0.25	2.77 ± 0.22	2.54 ± 0.23	1.17 ± 0.21	1.28 ± 0.17	1.11 ± 0.13	2.02 ± 0.11	2.41 ± 0.17	2.69 ± 0.13	1.09 ± 0.26	1.10 ± 0.35	1.01 ± 0.18
NA (mmol/L)	144 ± 1	142 ± 2	143 ± 1	143 ± 1	143 ± 1	143 ± 1	143 ± 2	142 ± 1	141 ± 0	142 ± 1	143 ± 1	143 ± 2
K (mmol/L)	4.5 ± 0.2	4.9 ± 0.4	4.7 ± 0.4	4.4 ± 0.4	4.3 ± 0.2	4.5 ± 0.4	3.9 ± 0.2	4.0 ± 0.1	4.1 ± 0.2	3.8 ± 0.2	3.8 ± 0.4	3.9 ± 0.2
CL (mmol/L)	101 ± 1	100 ± 2	100 ± 1	103 ± 2	103 ± 1	103 ± 2	103 ± 2	101 ± 1	101 ± 1	103 ± 1	104 ± 2	104 ± 3
Hematology												
WBC × 10^9/L	18.86 ± 1.13	13.7 ± 3.3	14.51 ± 4.93	9.95 ± 3.1	9.49 ± 2.66	10.03 ± 2.54	11.16 ± 3.92	11.39 ± 3.96	10 ± 1.45	5.79 ± 1.19	6.34 ± 1.68	5.93 ± 1.41
NEUT × 10^9/L	1.6 ± 0.47	1.52 ± 0.6	1.24 ± 0.48	1.22 ± 0.39	1.21 ± 0.45	1.26 ± 0.33	1.17 ± 0.58	0.58* ± 0.17	0.6 ± 0.19	0.52 ± 0.16	0.65 ± 0.24	0.61 ± 0.2
LYMPH × 10^9/L	11.86 ± 1.17	11.66 ± 2.6	12.67 ± 4.46	8.28 ± 2.7	7.87 ± 2.4	8.33 ± 2.45	9.62 ± 3.19	12.41 ± 3.75	8.96 ± 1.19	5.01 ± 1.07	5.41 ± 1.52	5.05 ± 1.28
MONO × 10^9/L	0.31 ± 0.05	0.27 ± 0.11	0.35 ± 0.21	0.21 ± 0.1	0.17 ± 0.09	0.18 ± 0.07	0.16 ± 0.1	0.14 ± 0.03	0.22 ± 0.08	0.11 ± 0.05	0.11 ± 0.04	0.1 ± 0.04
EOS × 10^9/L	0.31 ± 0.05	0.1 ± 0.01	0.09 ± 0.04	0.13 ± 0.06	0.13 ± 0.04	0.13 ± 0.04	0.09 ± 0.03	0.11 ± 0.04	0.09 ± 0.03	0.1 ± 0.02	0.09 ± 0.04	0.1 ± 0.02
BASO × 10^9/L	0.06 ± 0.01	0.06 ± 0.04	0.07 ± 0.03	0.03 ± 0.02	0.03 ± 0.02	0.03 ± 0.02	0.04 ± 0.03	0.06 ± 0.03	0.03 ± 0.01	0.02 ± 0.01	0.02 ± 0.01	0.01 ± 0
LUC × 10^9/L	0.09 ± 0.04	0.09 ± 0.03	0.1 ± 0.05	0.08 ± 0.05	0.09 ± 0.04	0.09 ± 0.03	0.08 ± 0.05	0.1 ± 0.05	0.1 ± 0.03	0.05 ± 0.02	0.06 ± 0.04	0.05 ± 0.01
RBC × 10^{12}/L	6.35 ± 0.2	6.66* ± 0.11	6.62* ± 0.14	8.15 ± 0.37	8.3 ± 0.44	8.48 ± 0.33	6.67 ± 0.18	6.66 ± 0.46	6.51 ± 0.19	7.8 ± 0.16	7.68 ± 0.32	7.74 ± 0.25
HGB (g/dL)	12.7 ± 0.3	13.2 ± 0.4	13.2 ± 0.3	14.2 ± 0.6	14.4 ± 0.5	14.4 ± 0.5	13 ± 0.4	13.4 ± 0.7	12.7 ± 0.5	14 ± 0.4	14 ± 0.4	14 ± 0.5
HCT (L/L)	0.397 ± 0.008	0.412 ± 0.015	0.412 ± 0.005	0.438 ± 0.015	0.448 ± 0.013	0.446 ± 0.014	0.392 ± 0.016	0.407 ± 0.021	0.384 ± 0.017	0.425 ± 0.013	0.421 ± 0.014	0.427 ± 0.01
MCV (fL)	62.4 ± 1.7	61.9 ± 1.6	61.9 ± 0.9	58.8 ± 1.9	54 ± 1.6	52.6 ± 1.2	58.7 ± 1.9	61.2 ± 2.8	59 ± 2.3	54.5 ± 1.7	54.8 ± 0.9	55.2 ± 1.7

(*Continued on next page*)

Genzyme Ex. 2020
Sarepta Therapeutics, Inc. v. Genzyme Corporation
Page 7 of 18

Table 1. *Continued*

	Males					Females				
	Day 8			Day 91		Day 8			Day 91	
MCH (pg)	19.9 ± 0.5	19.8 ± 0.5	19.9 ± 0.2	17.5 ± 0.5	17.4 ± 0.4	17 ± 0.6	19.5 ± 0.5	20.2 ± 0.8	19.5 ± 0.6	18 ± 0.5	18.2 ± 0.4	18.1 ± 0.4
MCHC (g/dL)	31.9 ± 0.1	31.9 ± 0.3	32.2 ± 0.6	32.5 ± 0.7	32.2 ± 0.5	32.3 ± 0.5	33.2 ± 0.4	33 ± 0.3	33 ± 0.5	33 ± 0.4	33.2 ± 0.4	32.9 ± 0.5
RDW (%)	12.5 ± 0.2	13.1 ± 0.5	12.9 ± 0.6	13.6 ± 1.6	13.8 ± 0.9	13.9 ± 0.8	11.8 ± 0.3	11.3 ± 0.2	12.1 ± 0.7	11.5 ± 0.4	11.6 ± 0.3	11.4 ± 0.3
PLT × 10^9/L	947 ± 123	917 ± 88	878 ± 49	861 ± 186	955 ± 86	830 ± 217	985 ± 28	982 ± 105	972 ± 63	782 ± 84	754 ± 142	803 ± 78
RETIC × 10^9/L	410.7 ± 38	434 ± 73.6	452.3 ± 91.1	262.4 ± 114.8	256.6 ± 74.9	253.6 ± 58.1	292.6 ± 67	285.4 ± 54.8	329.9 ± 90	172.1 ± 35.7	178.1 ± 34	170.3 ± 37.1

See the Materials and Methods for details on the design of the GLP toxicology and biodistribution study. For all parameters, n = 5 for day 8 and n = 10 for day 91; vehicle group at day 91 n = 9. Datasets are reported as mean ± SD. 1× corresponds to animals injected with 5×10^{12} vg/kg (ss)AAV8-hUGTA1; 5× corresponds to animals injected with 2.5×10^{13} vg/kg (ss)AAV8-hUGTA1. *Significantly different from control group (vehicle), p value ≤ 0.05 (Dunnet).

AAV8 capsid starting at day 8 and regardless of the dose infused (Table 2). Some animals also developed binding immunoglobulin G (IgG) against the hUGT1A1 protein (Table 2). To understand the origin of this response, we measured the formation of anti-transgene antibodies in Ugt1$^{-/-}$ deficient mice treated with AAV8 vector carrying the mouse UGT1A1 transgene (mUGT1A1). TB in plasma, transgene expression, and humoral response directed against the transgene were assessed. Long-term correction of TB was observed in both male and female animals (Figure 7A), along with vg persistence (Figure S6A) and UGT1A1 protein expression in the liver of treated animals (Figure 7B; Figure S6B). No anti-mUGT1A1-binding antibodies were detected in the plasma of treated mice 1 month post-injection, while 3 of 4 of the mice dosed with the human construct (hUGT1A1) had detectable antibodies (Table 3).

Similar results were obtained in Gunn rats. AAV8-UGT1A1 vectors encoding for both human and rat transgenes corrected plasma TB (Figure 7C). VGCN analysis demonstrated that the two vectors transduced hepatocytes (Figure S6C), and a similar expression of the UGT1A1 protein was observed (Figure S6D). Anti- hUGT1A1-binding antibodies were measured by ELISA (Figure 7D), and anti-rat UGT1A1-binding antibodies were measured by western blot (Figure 7E). Also in this case, the species-specific version of the UGT1A1 transgene appeared to be less immunogenic than the human counterpart (Table 3).

These results indicate that the hUGT1A1 transgene elicits humoral responses in rodents, supporting the use of species-specific transgenes to more carefully assess transgene immunogenicity.

The Administration of Glucocorticoids in Conjunction with (ss)AAV8-hUGT1A1 Gene Transfer Is Safe in Mouse and Rat Models of CN Syndrome

An immune response triggered by AAV is a potential concern for gene therapy clinical applications, and, based on the experience with AAV8-mediated liver gene transfer for hemophilia B, it is known that a short course of corticosteroids may be needed to control the immune response directed against the vector.[11,12]

To identify possible interactions of corticosteroids with AAV gene transfer in CN animals, we used both Gunn rats and Ugt1$^{-/-}$ mice. In Gunn rats, a tapering course of corticosteroid was given 4 weeks after gene transfer. No detrimental effect on the correction of TB levels was observed (Figure 8A). Accordingly, no effect of methylprednisolone treatment on VGCN was noted (Figure 8B), and no obvious treatment-related effects on transaminase activities were measured (Figure S7A). Similar experiments were performed in adult Ugt1$^{-/-}$ mice, treated daily with methylprednisolone starting 1 day before vector administration (Figure 8C). No adverse effects were noted following methylprednisolone treatment, as the correction of TB levels with (ss)AAV8-hUGT1A1 was achieved in mice with or without corticosteroids (Figure 8D). Accordingly, liver enzymes in methylprednisolone-treated and control mice remained unchanged (Figure S7B). Histological analysis of the liver 9 months post-injection

Genzyme Ex. 2020
Sarepta Therapeutics, Inc. v. Genzyme Corporation
Page 8 of 18

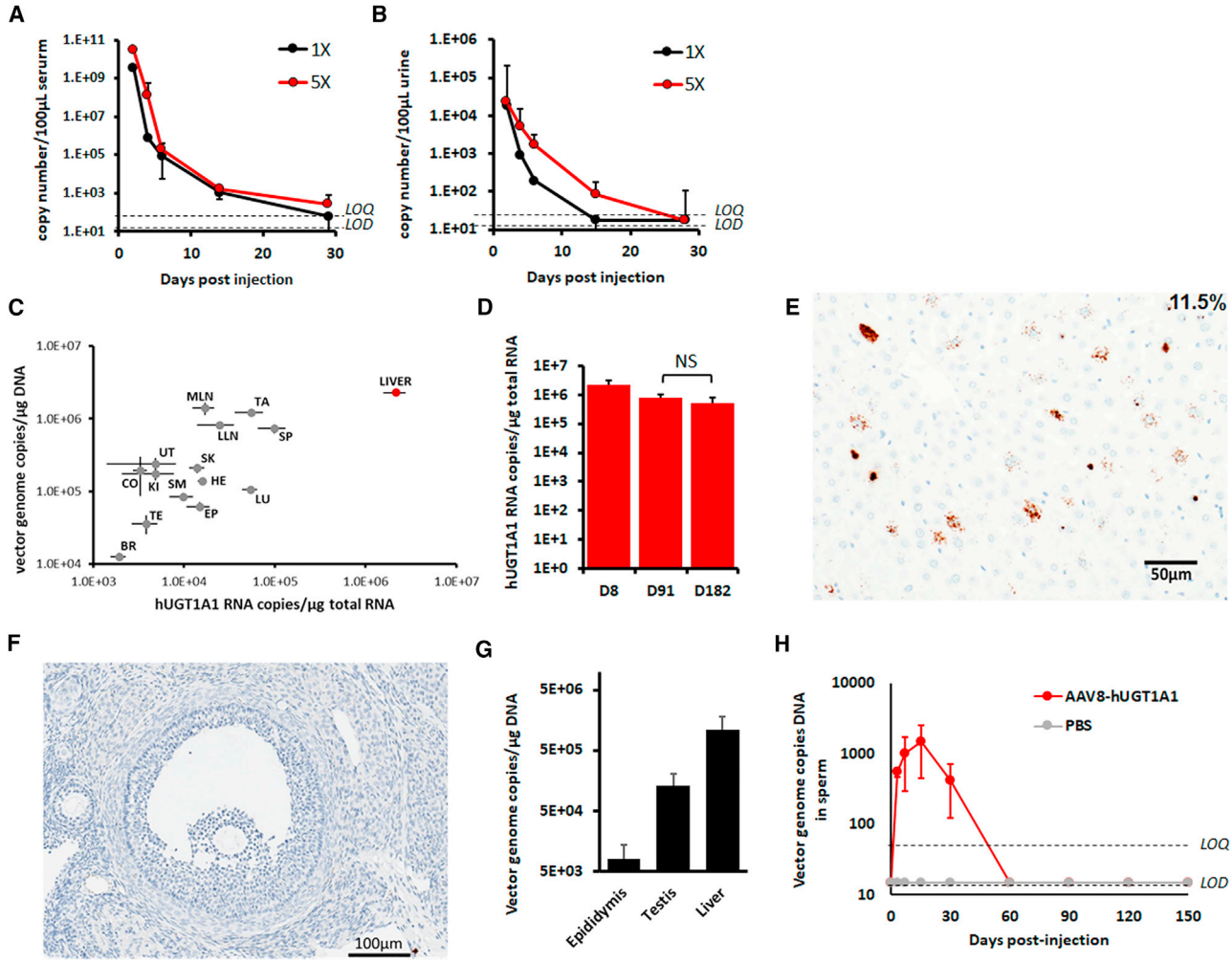

Figure 6. (ss)AAV8-hUGT1A1 Vector Shedding and Biodistribution

(A–D) Male and female Sprague-Dawley rats were injected with 5×10^{12} vg/kg (1×) or 2.5×10^{13} vg/kg (5×) (ss)AAV8-hUGT1A1 vector produced in suspension at large scale (200 L). Vector shedding in fluids collected from day 2 to day 29 is shown. Vector genome copy number was detected in serum (A) and urine (B). Limit of detection (LOD) and limit of quantification (LOQ) of the assay are indicated. (C) Correlation of vector genome copy number and hUGT1A1 mRNA expression in different tissues obtained from animals injected with (ss)AAV8-hUGT1A1 vector at 2.5×10^{13} vg/kg. (D) hUGT1A1 mRNA expression measured in liver 8, 91, and 182 days after vector injection. Mean ± SD is shown. Statistical analyses were performed by ANOVA (NS, not significant). (E and F) *In situ* hybridization analysis of hUGT1A1 mRNA in liver (E) or ovary (F) of rats injected with (ss)AAV8-hUGT1A1 vector at 2.5×10^{13} vg/kg. (G and H) Male rabbits were injected with 5×10^{12} vg/kg (ss)AAV8-hUGT1A1 vector or PBS. (G) Vector genomes were quantified by qPCR in epididymis, testis, and liver samples collected at day 150. Mean ± SD are shown. (H) Vector shedding in sperm collected from day 3 to day 150. Mean ± SD of vector genome copy number detected in sperm is shown. Limit of detection (LOD) and limit of quantification (LOQ) of the assay are indicated.

showed no major abnormalities in mice treated with corticosteroids compared to their controls (Figures S7C–S7G). Finally, a molecular analysis of VGCN showed no significant effect of corticosteroid on liver transduction (Figure 8E; $p = 0.1608$, sham versus methylprednisolone [MePRDL]).

These results demonstrate the safety of glucocorticoid administration concomitant to gene transfer in animal models of CN syndrome.

DISCUSSION

Gene therapy with AAV vectors holds the potential for a curative treatment for several liver metabolic disorders.[10] Among them, CN syndrome appears to be an ideal candidate.[8]

Here we propose the use of a (ss)AAV8 vector driving the liver-specific expression of hUGT1A1 for the safe and efficient correction of hyperbilirubinemia, the pathological hallmark of CN syndrome.

Genzyme Ex. 2020
Sarepta Therapeutics, Inc. v. Genzyme Corporation
Page 9 of 18

Table 2. GLP Toxicology Study: Humoral Immune Response against AAV8 Capsid and hUGT1A1 Transgene

Vector Dose	Baseline	Day 8	Day 29	Day 91	Day 182
Anti-AAV8 Capsid Binding IgG (mean ± SD; μg/mL)					
Low dose	0 ± 0.1	38.9 ± 11.3	539.3 ± 161	709.1 ± 16.8	–
High dose	0.1 ± 0.2	26.9 ± 11.8	631.4 ± 93.4	670.7 ± 39.7	1,035.9 ± 470.5
UGT1A1 Transgene Binding IgG (mean ± SD; μg/mL)					
Low dose	0.3 ± 0.5	0.5 ± 0.7	2.4 ± 1.3	16.1 ± 11.9	–
High dose	0.1 ± 0.2	0.7 ± 0.5	3.5 ± 4.2	11.7 ± 8.3	11.8 ± 7.7

Detection of humoral response directed against capsid and transgene in rat plasma. See the Materials and Methods for details on the design of the GLP toxicology and biodistribution study.

To select the best candidate for clinical development, we compared an (sc)AAV8 vector designed for the expression of hUGT1A1 with an optimized (ss)AAV8 vector.[19] (sc)AAV and (ss)AAV vectors have been used to transduce the liver in the context of several genetic disorders.[10] To this aim, the use of (sc)AAV vectors could provide potential advantages related to the bypass of the step of double-stranded DNA (dsDNA) conversion of the vg, thus facilitating the viral transduction.[28] However, the use of (sc)AAV vectors has potential drawbacks, including the reduced genome-packaging capacity, the lower vector production yields, and the low homogeneity (at least in the context of the current study) due to the production of vectors containing truncated genomes. Hence, here we carefully characterized (sc)AAV8-hUGT1A1 and (ss)AAV8-hUGT1A1 vectors, and we showed that, using a research-grade production method, (ss)AAV8-hUGT1A1 vectors were generated with higher yields and superior product homogeneity.

Several studies have been published in which both (sc)- and (ss)AAV vectors were used to transduce the human liver; these include trials for hemophilia B,[12,13,29] hemophilia A,[14] and acute intermittent porphyria.[30] In the present work, we demonstrated, in the Gunn rat model of CN, that the clinical candidate (ss)AAV8-hUGT1A1 vector has a similar potency as an (sc)AAV vector carrying the same transgene, both in terms of therapeutic efficacy and liver transduction level. One caveat of the current work is that, due to the size of the UGT1A1 transgene and the reduced genome-packaging capacity of (sc)AAVs (~2.5 kb), the expression cassettes of the (ss)- and (sc)AAV8-hUGT1A1 vectors were not identical. Future studies with vectors carrying exactly the same expression cassettes will help to more carefully compare the potency of vectors carrying different genome configurations.

Considerations over the ability to produce (sc)AAV vectors in sufficient quantity and of acceptable quality, and concerns over the potential higher immunogenicity of these vectors,[31] prompted us to focus on an (ss)AAV8-hUGT1A1 vector to develop a scalable production process specific for this vector construct. A scalable animal product-free good manufacturing practice (GMP)-compliant process for (ss)AAV8-hUGT1A1 vector production was developed. The process consisted of transient tri-transfection of HEK293 cells cultured in suspension in bioreactors,[32] which was able to supply vector in sufficient quantities to support preclinical and clinical development of the investigational gene therapy candidate.

One difference between the suspension manufacturing method and the research-grade production system used in this study resides in the downstream process, which in the suspension process consists of a scalable column-based affinity purification technique, no longer efficient in eliminating the empty particles in the final product. As already highlighted,[33] the consequences of the presence of empty capsids in the final product remain unclear, although preparations of AAV vectors containing both capsid species have been safely used in several liver gene transfer clinical trials.[11–15] Additionally, it has been shown that the optimization of the ratio of full to empty capsids in the final formulation of the therapeutic vector could maximize the efficacy of gene transfer,[34] as the empty capsids can act as decoys for anti-AAV-neutralizing antibodies. Here we compared the potency of (ss)AAV8-hUGT1A1 vectors generated with two production methods, one leading to full AAV particles only and the other leading to a mix of empty and full capsids. We demonstrated a similar potency of the two vector preparations both *in vitro* and *in vivo*. We showed that the (ss)AAV8-UGT1A1 vectors produced in suspension and containing empty particles efficiently corrected hyperbilirubinemia in CN mice and reached similar liver transduction levels when compared to research-grade vector preparations composed of full particles only.

One important aspect of the current study is that it validates the rat as an ideal model of liver gene transfer. Through a careful comparison of the AAV vector liver transduction efficiency in rats and mice, we provided evidence that the efficiency of liver transduction of AAV8 vectors in rats is similar to that expected in humans. Conversely, AAV8 vectors transduce the mouse liver with at least a log higher efficiency, thus potentially overstating the therapeutic efficacy of a gene therapy drug candidate. Accordingly, using an (ss)AAV8-hFIX vector, we observed lower liver transduction in Gunn rats than in mice. At the same vector dose (5×10^{12} vg/kg), hFIX transgene expression levels detected in the blood of mice were ~100% of those measured in humans. Conversely, the injection of the same vector dose in rats resulted in levels of hFIX in the same range of those described in humans receiving a comparable vector dose (2×10^{12} vg/kg) of a similar AAV8 vector encoding for hFIX.[11,12] These data support the concept that, when available, rats are animal models suitable for dose-finding studies, in particular for AAV8 vectors, and their use in the current study provided a valuable tool to support the choice of a starting dose of vector to be used in the clinic, which holds the prospect of driving therapeutic efficacy in humans.

Efforts were then focused on the manufacturing process scale-up. (ss)AAV8-hUGT1A1 vectors were produced at a 200-L scale. Vector preparations were carefully analyzed for both the content of full and empty capsids and DNA contaminants, among others. Notably, for the determination of empty-to-full capsid ratio, here we used AUC,

Genzyme Ex. 2020
Sarepta Therapeutics, Inc. v. Genzyme Corporation
Page 10 of 18

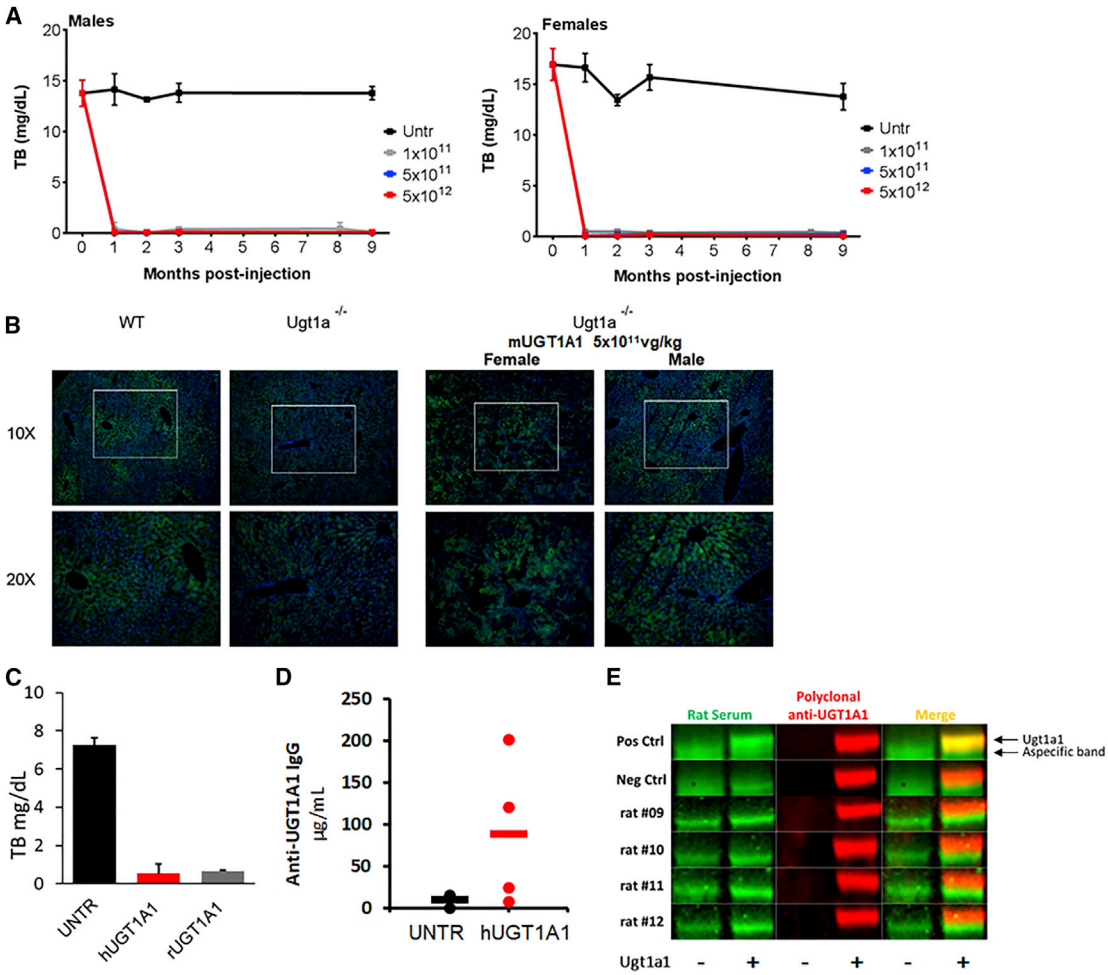

Figure 7. Assessment of Immunogenicity of Species-Specific UGT1A1 in Two Animal Models of CN

(A and B) Ugt1$^{-/-}$ mice (P60) were injected i.p. with PBS (UNTR) or (ss)AAV8-UGT1A1 vectors coding for mouse transgene at 1 × 10^{11} vg/kg, at 5 × 10^{11} vg/kg, or 5 × 10^{12} vg/kg. (A) Plasma bilirubin determination in male and female Ugt1$^{-/-}$ mice after treatment with different doses of AAV8-mUGT1A1 vectors. (B) Immunofluorescence analysis of representative liver sections from WT, Ugt1$^{-/-}$ untreated, and treated with 5 × 10^{11} vg/kg vector dose. Rectangles indicate magnification images shown below. 1 × 10^{11}dose, male n = 5 and female n = 3; 5 × 10^{11} dose, male n = 3 and female n = 4; 5 × 10^{12} dose, male n = 3 and female n = 4. (C–E) 8-week-old Gunn rats were injected intravenously with PBS (UNTR) or 5 × 10^{12} vg/kg (ss)AAV8-UGT1A1 vector encoding for human UGT1A1 (hUGT1A1) or rat UGT1A1 (rUGT1A1). (C) TB levels in plasma of rats analyzed 186 days post-treatment. Data are plotted as mean ± SD. Statistical analyses were performed by ANOVA (NS, not significant). (D and E) Anti-UGT1A1 IgG analyzed 186 days post-treatment by ELISA for hUGT1A1 (D) or by western blot for rUGT1A1 (E). Rat livers expressing rUGT1A1 (+) or not (–) were loaded. Individual serum of rat treated with (ss)AAV8-rUGT1A1 (green) or commercial anti-UGT1A1 antibody (red) was used to detect UGT1A1 protein.

a method that has been demonstrated to provide a reliable readout.[35,36]

GLP-compliant biodistribution studies confirmed the expected tissue distribution of AAV8 vectors. However, due to the low-level persistence of vgs in gonads 6 months post-vector infusion, a germline transmission study was performed in male rabbits. As already reported in animal models and humans,[11,12,37] vector was transiently detected in the sperm of rabbits, indicating a negligible risk of germline transmission that could be further mitigated by physical barrier contraception during the clinical trial. Similarly, ISH studies in female rats confirmed that AAV vectors do not transduce efficiently oocytes, as previously shown using a reporter vector.[38]

In our GLP toxicology and biodistribution study, all animals developed a significant humoral immune response against the AAV8 capsid, a result that is largely expected.[39] Some animals also developed IgG against the hUGT1A1 protein. Development of anti-hUGT1A1 antibodies has been also documented following the administration of AAV-hUGT1A1,[18] in studies conducted in CN rats, with no consequence on the vector efficacy.[19] The development of anti-hUGT1A1 antibodies is not considered as toxicologically relevant, as no elevations of transaminases or treatment-related histopathological

Genzyme Ex. 2020
Sarepta Therapeutics, Inc. v. Genzyme Corporation
Page 11 of 18

Table 3. Testing of Species-Specific UGT1A1 Transgene Immunogenicity

	Number of Animals Positive for Anti-UGT1A1 IgG/Total	
UGT1A1 Transgene	Mice	Rats
Human	3/4	2/4
Mouse	0/4	not tested
Rat	not tested	0/4

findings were noted in the GLP toxicity study. Nevertheless, we further investigated the origin of this finding by testing whether the immune response was driven by the human transgene expressed in rats. To this aim, we injected rat and mouse UGT1A1 transgenes in the corresponding rat and mouse models of CN syndrome. The absence of humoral response directed against rat UGT1A1 in Gunn rats and mouse UGTA1 in the $Ugt1^{-/-}$ mouse model suggests that the anti-hUGT1A1 antibodies observed in the GLP study in rats originated from species-specific transgene immunogenicity. One important implication of this work is that it indicates that immune responses observed in animal models may be driven by species-specific reactions to the transgene expressed, which in some cases may confound the readout of preclinical studies.

Finally, as glucocorticoids have been used to modulate vector immunogenicity in several trials,[11–15,40] here we tested the safety of the approach in the context of CN syndrome. Immunosuppression can indeed affect the safety and efficacy of gene transfer;[41,42] we demonstrated in two animal model of CN syndrome that methylprednisolone administration had no impact on the safety and efficacy of the gene therapy.

In conclusion, this work describes the development of an investigational gene therapy for CN syndrome based on an AAV8 vector injected intravenously to deliver a corrected copy of the UGT1A1 gene to hepatocytes. The vector construct has been optimized for liver-restricted expression, and it is based on a gene delivery platform with a proven excellent safety and efficacy profile in humans. We showed successful and efficient manufacturing scale-up, and we described a comprehensive approach to safety and efficacy in preclinical studies. This work constitutes the basis for the initiation of an AAV-mediated gene therapy clinical trial in CN.

MATERIALS AND METHODS

Plasmid Construct

The transgene expression cassette of the (ss)AAV8-hUGT1A1 carrying a codon-optimized cDNA sequence encoding for hUGT1A1 was previously described.[19] This construct (also known as GNT0003) was selected as the clinical candidate (ClinicalTrials.gov: NCT03466463). The cassette contains the human hemoglobin beta (HBB)-derived synthetic intron (HBB2)[43] and the HBB polyadenylation signal. The transgene expression cassette of the (sc)AAV8-hUGT1A1 was developed by Dr. Bosma (Academic Medical Center, Amsterdam, the Netherlands), and it consisted of a codon-optimized cDNA sequence encoding for hUGT1A1 transgene cloned into an (sc)AAV backbone. This plasmid carries the AAV2 inverted terminal repeats (ITRs) with an intact 5′ terminal resolution site (trs) without the analogous 3′ trs, a hybrid liver-specific promoter (HLP), a modified SV40 small intron[44] sequence, and the SV40 late polyadenylation signal. For the *in vitro* comparison of hUGT1A1 expression levels, we used an (ss)AAV8-GFP as a control. The expression cassette contained the cDNA sequence encoding for EGFP transgene, the phosphoglycerate kinase (PGK) promoter, and an SV40 polyA sequence. For the *in vivo* comparative study between mice and rats, we used an (ss)AAV8 vector expressing coagulation factor IX under the transcriptional control of a liver-specific promoter.[45]

Production of AAV Vectors

Research-grade AAV vectors used in this study were produced using a slight modification of the adenovirus-free transient transfection methods described. Briefly, adherent HEK293 cells grown in roller bottles were transfected with the three plasmids containing the adenovirus helper proteins, the AAV Rep and Cap genes, and the ITR-flanked transgene expression cassette. At 72 h after transfection, cells were harvested, lysed by sonication, and treated with Benzonase (Merck-Millipore, Darmstadt, Germany). Vectors were then purified using two successive ultracentrifugation rounds in cesium chloride density gradients. Full capsids were collected, and the final product was formulated in sterile PBS containing 0.001% Pluronic (Sigma-Aldrich, St. Louis, MO) and stored at −80°C. GMP-like (ss)AAV8-hUGT1A1 vectors used in this study were produced in a bioreactor and at different scales up to 200 L by adenovirus-free transient transfection method. Suspension HEK293 cells were transfected with PEI (PEIpro, Polyplus) with the three same plasmids mentioned above. At 24 h after transfection, cells were treated with Benzonase, and, 2 days later, they were lysed with Triton (Sigma, St. Louis, MO) and clarified by filtration. Vectors were purified by a single chromatography column based on AVB Sepharose immuno-affinity (GE Healthcare) before concentration by tangential flow filtration. Purified particles were formulated in Ringer-Lactate solution containing 0.001% Pluronic (F68), vialed, and stored at −80°C.

Characterization of AAV Vectors

Titers of AAV vector stocks were determined using real-time qPCR. Specific probe and primers were as follows: forward, 5′-GGC GGGCGACTCAGATC-3′; reverse, 5′-GGGAGGCTGCTGGTGAA TATT-3′; and probe, 5′-AGCCCCTGTTTGCTCCTCCGATAA CTG-3′.

To perform alkaline agarose gel, viral DNA was extracted from 100 μL AAV solutions. Samples were denatured 5 min at 95°C and prepared in 6× alkaline-loading buffer (300 mM NaOH, 6 mM EDTA, 18% Ficoll, 0.5% bromocresol green, and 0.25% xylene cyanol) and GelRed1X. After electrophoresis in denaturing conditions (50 mM NaOH-1 mM EDTA), gel was stained with GelRed diluted 1:10,000.

AUC measures the sedimentation coefficient of macromolecules by following over time the optical density of a sample subjected to

Genzyme Ex. 2020
Sarepta Therapeutics, Inc. v. Genzyme Corporation
Page 12 of 18

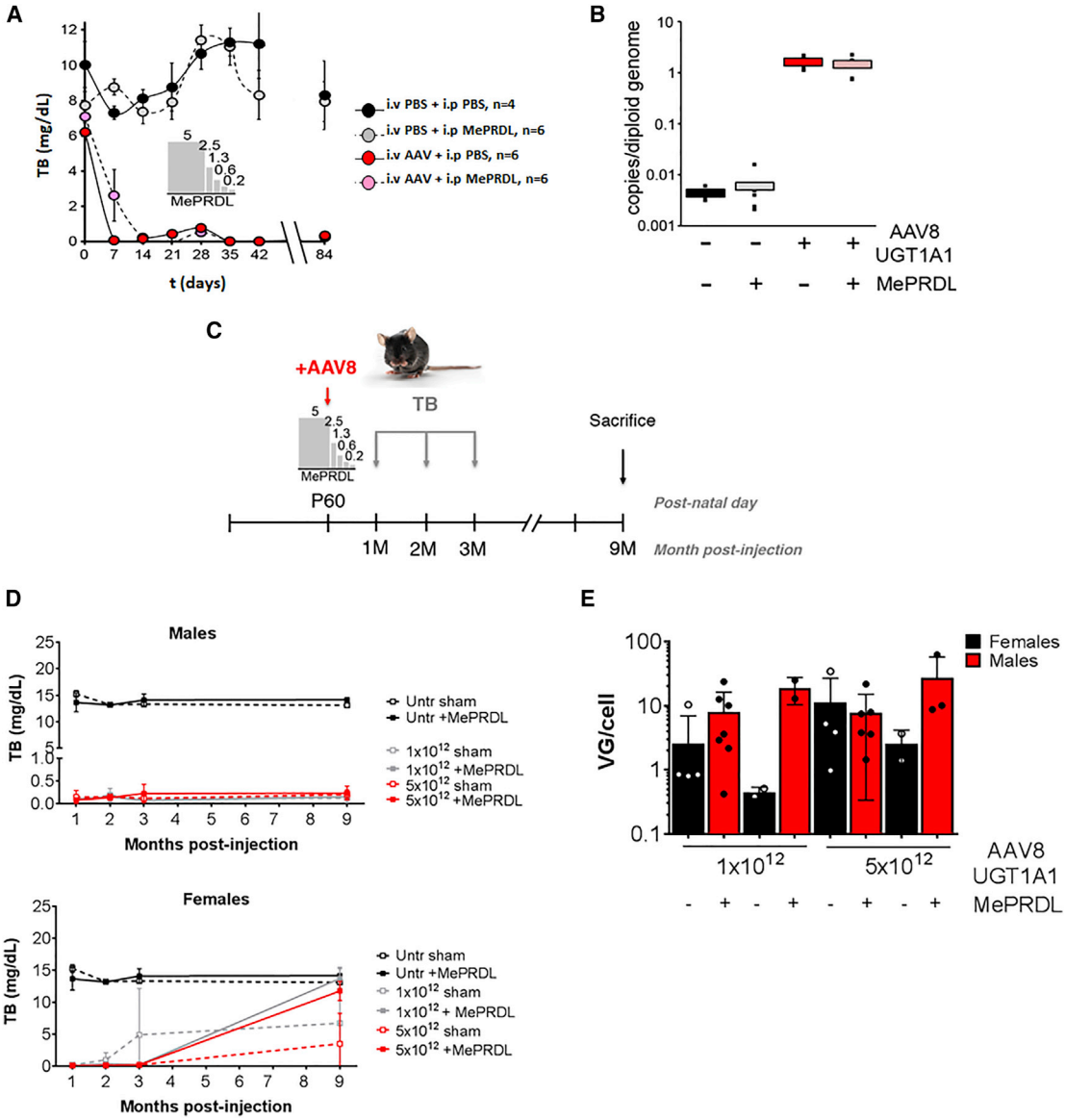

Figure 8. Corticosteroid Treatment in CN Animal Models Does Not Affect Gene Transfer Efficacy

(A and B) Gunn rats were injected with PBS (black) or 5×10^{12}vg/kg (ss)AAV8-UGT1A1 (red) at day 0. At 1 month after the treatment, a 15-day tapering dose of methylprednisolone was administered intraperitoneally in half of the rats (gray and pink). Rats were weekly bled and sacrificed 3 months after vector injection. (A) Total bilirubin (TB) levels were weekly measured and plotted versus time. Data are expressed as mean ± SE. The internal bar chart describes the tapering course of methylprednisolone (MePRDL). (B) Vector genome copy number (VGCN) per cell was measured by qPCR performed on genomic material extracted from livers of Gunn rats. Values were normalized for the number of copies of genomic DNA using titin as standard. In the figure are the single values measured (small black dots) and the median value for each treatment. (C–E) Ugt1$^{-/-}$ mice were injected as adults with the indicated doses (vg/kg). A MePRDL treatment was initiated the day before the injection of the AAV vector and lasted for 5 days at decreasing doses (5.0, 2.5, 1.3, 0.6, and 0.3 mg/kg). At 1, 2, and 3 months post-injection, mice were bled and TB levels in plasma were analyzed. At 9 months post-injection, mice were sacrificed and molecular analysis was carried out. (C) Experimental strategy. (D) TB levels in plasma in male and female Ugt1$^{-/-}$ mice after treatment with different doses (vg/kg) of rAAV8-mUGT1A1 with or without corticosteroids. (E) VGCN in male and female mice 9 months post-injection. Results are expressed as mean ± SD and individual values are plotted. 1×10^{12} dose, male sham n = 7, male + MePRDL n = 2, female sham n = 5, and female + MePRDL n = 2; 5×10^{12} dose, male sham n = 6, male + MePRDL n = 3, female sham n = 4, and female + MePRDL n = 2.

ultracentrifugation. The difference in the sedimentation coefficient, measured by Raleigh interference or 260-nm absorbance, depends on the content of viral genome in the capsid. AUC analysis was performed using a Proteome Lab XL-I (Beckman Coulter, Indianapolis, IN). 400 μL AAV vector and 400 μL formulation buffer were loaded into a two-sector velocity cell. Sedimentation velocity centrifugation

Genzyme Ex. 2020
Sarepta Therapeutics, Inc. v. Genzyme Corporation
Page 13 of 18

was performed at 20,000 rpm and 20°C. Absorbance (260 nm) and Raleigh interference optics were used to simultaneously record the radial concentration as a function of time until the lightest sedimenting component cleared the optical window (approximately 1.5 h). Absorbance data required the use of extinction coefficients to calculate the molar concentration and the percent value of the empty and genome-containing capsids. Molar concentrations of both genome-containing and empty capsids were calculated using Beer's law, and percentages of full genome-containing and empty capsids were calculated.

For the characterization of the VP protein content in the different populations of particles, AAV8-hUGT1A1 vectors were loaded in cesium chloride solution (1.38 g/cm^3) and ultracentrifuged at 38,000 rpm and 20°C for 40 h. The total volume of the viral/cesium solution was then collected in 16 fractions (0.5 mL). The CsCl was removed from the fractions by repeated dialysis cycles against PBS-0.001% pluronic F68 solution. A volume of 10 μL of each fraction was loaded onto a 4%–12% SDS-polyacrylamide gel (Thermo Fisher Scientific, Waltham, MA). After protein migration, the gel was stained with a SYPRO Ruby solution (Invitrogen, Carlsbad, CA).

hUGT1A1 Expression in Huh7 Cell Line

For transduction experiments, six-well plates containing 80% confluent Huh-7 cells were transduced with AAV8-UGT1A1 vectors at the indicated MOI. AAV8-GFP-transduced cells were included as a control. At 72 h after transduction, cells were harvested and frozen at −20°C until processing. Microsome extraction was performed at 4°C. Frozen cell pellets were resuspended in 300 μL lysis buffer (20 mM HEPES and 1% Triton X-100) and protease inhibitor cocktail (Sigma-Aldrich, St. Louis, MO) and centrifuged 5 min at 100 × *g*. Supernatants were collected and centrifuged 60 min at 18,000 × *g*. Pellets were resuspended in 100 μL 20 mM HEPES, and the protein concentration was determined using the BCA Protein Assay kit (Thermo Fisher Scientific, Waltham, MA), following the manufacturer's instructions. Microsomal extracts were separated on a 4%–12% bis-tris polyacrylamide gel (Thermo Fisher Scientific, Waltham, MA). The same amount of protein was loaded in each lane. The gel was transferred onto a nitrocellulose membrane and blotted with an anti-UGT1A1 antibody (Santa Cruz Biotechnology, Santa Cruz, CA) and an anti-actin antibody (Sigma-Aldrich, St. Louis, MO), used as a loading control. The secondary antibodies and detection system were from LI-COR Biosciences (Lincoln, NE).

Animal Experiments

Ugt1$^{-/-}$ mice have been described previously.[16] WT or Ugt1$^{-/-}$ untreated littermates were used as controls as indicated. Mice were housed and handled according to institutional guidelines, and experimental procedures were approved by the International Centre for Genetic Engineering and Biotechnology board. Animals used in this study were at least 99.8% C57BL/6 genetic background, obtained after more than 9 backcrosses with WT C57BL/6 mice. Mice were kept in a temperature-controlled environment with 12-/12-h light-dark cycle. They received a standard chow diet and water *ad libitum*.

The Gunn rat is a naturally occurring model of CN syndrome that has no residual UGT1A1 enzyme activity. Rats and WT C57BL/6 mice used in this study were fed *ad libitum*, and they were housed and handled according to institutional guidelines. All *in vivo* experimental procedures were approved by the French and Italian competent authorities and Ethical Committees (ref. 2013007C and 2017002B_APAFIS#9667), according to the European Directive 2010/63/EU.

Both male and female animals were used to better represent the CN patient population, which includes both male and female individuals.

Gene Transfer Procedures and Phototherapy Treatment

Ugt1$^{-/-}$ Mice

Post-natal day 11 (P11) mice were intraperitoneally injected with AAV vectors or saline. Newborns were exposed to blue fluorescent light (Philips, Amsterdam, the Netherlands) for 12 h per day (synchronized with the light period of the light-dark cycle) up to 12 days after birth, and then they were maintained under normal light conditions. Intensity of the blue lamps was monitored monthly with an Olympic Mark II Bili-Meter (Olympic Medical, Port Angeles, WA). For adult studies, Ugt1$^{-/-}$ animals were exposed to blue fluorescent lamps up to day 20 after birth, as previously described.[20] Blood samples were collected at sacrifice by facial vein exsanguination. Liver tissues were collected at sacrifice for transgene expression assessment. For immunogenicity study and glucocorticoid administration evaluation, PBS or AAV vectors were administrated in adult (P60–P90) Ugt1$^{-/-}$ mice by intravenous injection in retro-orbital sinus. Blood samples and liver tissues were collected at sacrifice for transgene expression assessment.

Gunn Rats

6- to 8-week-old rats were injected intravenously via the tail vein with AAV vectors or saline. Blood samples were collected by retro-orbital venipuncture every week after AAV injection. To determine transgene expression, liver tissues were collected at sacrifice. For analysis of bilirubin glucuronides, bile samples were collected in this experiment at 3 months post-injection.

C57BL/6 Mice

The 6- to 8-week-old mice were injected intravenously via the tail vein with AAV vectors or saline. Blood samples were collected by retro-orbital venipuncture and liver tissues were collected at sacrifice.

Bilirubin Measurement

TB determination in mice and rats was performed in plasma as previously described. Plates were read at 560 nm on an Enspire plate reader (PerkinElmer, Waltham, MA). Bilirubin conjugates in bile were analyzed and quantified by high-performance liquid chromatography (HPLC) as previously described,[18] using an Omnisphere column (Varian, Palo Alto, CA) for the separation of bilirubin conjugates.[46]

Genzyme Ex. 2020
Sarepta Therapeutics, Inc. v. Genzyme Corporation
Page 14 of 18

hFIX Measurement

Levels of hFIX in plasma were quantified with an ELISA as described.[45] Capture antibody (Pierce Factor IX Antibody, MA1-43012) was used at 2.8 μg/mL, left overnight at 4°C, washed with PBS containing 0.05% Tween 20 (PBST), and blocked with 200 μL/well blocking buffer (6% milk in PBST) for 2 h at 37°C. Standards were prepared by serial dilutions of purified recombinant hFIX (starting concentration, 1,000 μg/mL). A horseradish peroxidase (HRP)-conjugated goat polyclonal anti-hFIX antibody (Affinity Biologicals, Ancaster, ON, Canada) diluted 1:1,000 was used as the secondary antibody.

Clinical Biochemistry

After prednisolone administration, the activities of alanine aminotransferase (ALT) and aspartate aminotransferase (AST) in rat plasma were measured on days 28, 35, 42, and 70 using colorimetric ALT and AST activity assay kits (Sigma, St. Louis, MO). Plates were read on an Enspire plate reader (PerkinElmer, Waltham, MA).

Virus VGCN Analysis

To reduce variability generated by the uneven transduction of liver parenchyma by AAV vectors, whole-rat livers were homogenized in 20 mM HEPES and 250 mM sucrose. For mouse samples, livers were harvested 1 month post-injection, pulverized in liquid nitrogen, and aliquoted for further molecular analysis. The following primers and probes were used: UGT1A1 forward 5′-GGCGGGCGACTCA GATC-3′, reverse 5′-GGGAGGCTGCTGGTGAATATT-3′; probe 5′-AGCCCCTGTTTGCTCCTCCGATAACTG-3′; titin forward 5′-AGAGGTAGTATTGAAAACGAGCGG-3′, reverse 5′-GCTAG CGCTCCCGCTGCTGAAGCTG-3′; probe 5′-TGCAAGGAAGCT TCTCGTCTCAGTC-3′. VGCN in mice was quantified by qPCR using specific primers for the hAAT promoter as previously described.[17]

Preparation of Total RNA, RT-PCR, and Real-Time PCR Analysis

Total RNA from mouse liver was prepared using EuroGOLD Trifast (Euroclone) according to the manufacturer's instructions. 1 μg total RNA was reverse transcribed using Moloney murine leukemia virus (M-MLV; Invitrogen, Carlsbad, CA) and oligodeoxythymidylic acid (oligodT) primer, according to the manufacturer's instructions. Total cDNA (1 μL) was used to perform either RT-PCR or qPCR using the following specific primers: forward, 5′-TAAATACGGACGAG GACAGG-3′; and reverse, 5′-ACCTCCTTGTGATTCCACAG-3′. qPCR was performed using iQTM SYBR Green Supermix (Bio-Rad, Hercules, CA) and a C1000 Thermal Cycler CFX96 Real Time System (Bio-Rad, Hercules, CA). Expression of the gene of interest was normalized to Gapdh housekeeping gene, using the following specific primers: forward, 5′-ATGGTGAAGGTCGGTGTGAA-3′; and reverse, 5′-GTTGATGGCAACAATCTCCA-3′. Real-time PCR data were analyzed using the ΔΔCt method.

Microsome Extraction and Western Blot Analysis

From 500 μL liver homogenate, microsome extraction was performed at 4°C. Rat liver samples were centrifuged 5 min at 100 × *g*, mixed with 4.5 mL 20 mM HEPES buffer, and centrifuged at 10,000 × *g* for 10 min. Supernatants were then centrifuged at 20,000 × *g* for 60 min. Pellets were resuspended in 400 μL 20 mM HEPES, and the protein concentration was determined using the BCA Protein Assay kit (Thermo Fisher Scientific, Waltham, MA), following the manufacturer's instructions. Microsomal extracts were separated on a 4%–12% bis-tris polyacrylamide gel (Thermo Fisher Scientific, Waltham, MA). The same amount of protein was loaded in each lane. The gel was transferred onto a nitrocellulose membrane and blotted with an anti-UGT1 rabbit polyclonal antibody (Santa Cruz Biotechnology, Santa Cruz, CA). Anti-actin (Sigma-Aldrich, St. Louis, MO) was used as a loading control. The secondary antibodies and detection system were from LI-COR Biosciences (Lincoln, NE).

For mouse samples, liver powder was homogenized in radioimmunoprecipitation assay (RIPA) buffer (150 mM NaCl, 1% NP-40, 0.5% DOC, 0.1% SDS, 50 mM Tris HCl [pH 8], and 2x protease inhibitors) and analyzed by western blot analysis, as described previously.[16]

GLP Toxicity/Biodistribution Study

This study was performed in Charles River (Tranent, UK) and Genosafe (Evry, France) laboratories. 100 5- to 7-week-old WT Sprague-Dawley rats were divided in 3 groups. Animals were treated either with (ss)AAV8-hUGT1A1 vector at 5×10^{12} vg/kg or at 2.5×10^{13} vg/kg or with PBS on day 0 by intravenous injection into the lateral tail vein. Follow-up of 3 weeks, 3 months, and 6 months was realized on the animals to evaluate the potential toxicity of the vector.

Clinical signs, body weight changes, food and water consumption, and clinical pathology parameters were evaluated during this study. For hematology, coagulation, clinical chemistry, urinalysis and immunogenicity assessment, and blood and urine samples were collected in each group at different time points from day 6 to the day of sacrifice. Urine and blood samples were also collected for the shedding analysis at days 2, 4, 6, 15, and 28 after injection. Gross necropsy findings, organ weights, biodistribution of the vector, and histopathologic examinations were conducted in animals euthanized 8, 91, and 182 days after vector administration.

GLP Germline Transmission Study

This study was performed in the Centre de Recherche Biologiques (CERB) (Baugy, France) and Genosafe (Evry, France) laboratories. Adult New Zealand White male rabbits were used for this study. (ss)AAV8-hUGT1A1 vectors or vehicle was administered once on day 1 by the intravenous route as a slow bolus over about 1 min in the marginal ear vein, in a volume of 0.9 mL/kg. Morbidity-mortality checks were performed twice daily. Clinical observations were performed before dosing and daily during the study. Body weights were recorded on days 1, 3, 5, 7, 9, and 15 and then once a week. Sperm samples were collected before dosing and on days 3, 7, 15, 30, 60, 90, 120, and 150. All animals were sacrificed on day 150. Selected organs (testis and epididymis, liver) were sampled on the day of necropsy and then analyzed for biodistribution assessment.

Genzyme Ex. 2020
Sarepta Therapeutics, Inc. v. Genzyme Corporation
Page 15 of 18

GLP ISH

This study was performed by Cytoxlab (Evreux, France). Briefly, the ISH method was automated and performed on formalin-fixed paraffin-embedded (FFPE) tissues. The sections were pre-treated by heating at +97°C for 24 min, and they were subsequently incubated with a protease for another 16 min at 37°C. The probes of interest (Advanced Cell Diagnostic, Newark, CA) were then hybridized at +43°C for 2 h. The amplification and detection systems were applied following the manufacturer's recommendations (RNAscope 2.5 VS, Advanced Cell Diagnostic, Newark, CA). The sections were stained with hematoxylin for 8 min and subsequently bluing reagent for 4 min. The slides were thoroughly washed in soapy water for 2 min, followed by running water for an additional 2 min. Finally, all slides were mounted.

Detection of Anti-AAV8 Antibodies in Rat Plasma

MaxiSorp 96-well plates (Thermo Fisher Scientific, Waltham, MA) were coated with AAV8 capsids in carbonate buffer at 4°C overnight. A standard curve of rat IgG (Sigma-Aldrich, St. Louis, MO) prepared as seven 2-fold dilution steps starting at 1 μg/mL was coated onto the wells. After blocking, plasma samples were added to plates and incubated 1 h at 37°C. Secondary antibody was added into the well (anti-Rat IgG-HRP), plates were developed with 3,3′,5,5′-tetramethylbenzidine substrate, and the optical density was assessed by spectrophotometry at 450 and 570 nm (for background subtraction) on Enspire plate reader (PerkinElmer, Waltham, MA) after blocking the reaction with 5% H_2SO_4.

Detection of Anti-UGT1A1 Antibodies in Rat Plasma

hUGT1A1

The same ELISA protocol as described above was followed but using, for this specific experiment, the UGT1A1 protein to coat the plates.

Rat UGT1A1

To detect antibodies against the rat UGT1A1 protein, 40 μg microsomal extracts from liver tissues expressing or not rat UGT1A1 transgene were separated on a 4%–12% bis-tris polyacrylamide gel (Thermo Fisher Scientific, Waltham, MA) and blotted onto a nitrocellulose membrane. Serum of each rat was used to develop a separate membrane as primary antibody (1:100). As a positive control, serum from rats immunized with UGT1A1 (1:200) and commercial anti-UGT1 rabbit polyclonal antibody (Millipore, Burlington, MA) were used. A positive signal, corresponding to the rat UGT1A1 (rUGT1A1) band, is detected only when antibodies against rUgt1a1 are present in the plasma of the animal. The secondary antibodies and detection system were from LI-COR Biosciences (Lincoln, NE).

Detection of Anti-UGT1A1 Antibodies in Mouse Plasma

The determination of anti-hUGT1A1 antibodies in mouse plasma has been described previously,[19,20] while the determination of anti-mouse UGT1A1 antibodies was performed with a minor modification of the previous protocol. The Huh7 cell line was infected with an AAV8 containing the mouse WT UGT1A1 cDNA (25,000 MOI), and 72 h later cells were harvested and total cell protein extract was prepared. 20 μg total protein extract derived from uninfected and AAV-infected cells was separated in a 10% SDS-PAGE, blotted onto nitrocellulose membrane. Plasma from individual animals was used as the primary antibody (1:200).

Methylprednisolone Treatment

Gunn Rats

6- to 8-week-old rats were divided into four groups. Animals were treated either with intravenous (ss)AAV8-hUGT1A1 vector or PBS on day 0. Later the rats were treated intraperitoneally (i.p.) daily with methylprednisolone (Solu-Medrol) or PBS utilizing the following schedule: 5 mg/kg prednisolone for 7 days, 2.5 mg/kg for the next 2 days, 1.3 mg/kg for the next 2 days, 0.6 mg/kg for the next 2 days, and 0.2 mg/kg for the last 2 days. The groups that received PBS on day 0 were treated with prednisolone or PBS between days 21 and 35. The groups that received rAAV8-hUGT1A1 vector on day 0 were treated with prednisolone or PBS between days 28 and 42. Blood samples were collected during the 3 months after AAV injection at several time points. Animals were sacrificed on day 84 and livers were collected.

Ugt1$^{-/-}$ Mice

Adult mice (8–12 weeks old) were injected retro-orbitally with (ss)AAV8-hUGT1A1 at the dose of 1×10^{12} or 5×10^{12} vg/kg. 1 day before the vector treatment, animals were treated i.p. with methylprednisolone (Solu-Medrol). Methylprednisolone was applied as five consecutive daily injections at the doses of 5.0, 2.5, 1.3, 0.6, and 0.2 mg/kg/day. Animals were sacrificed on day 84 and blood and liver were collected.

Histological Analysis of Liver Sections

At sacrifice, liver biopsies from AAV-treated animals and WT and Ugt1$^{-/-}$ untreated littermates were extracted and fixed with 4% paraformaldehyde (PFA) in PBS overnight at 4°C. The next day, biopsies were immersed in 20% sucrose in PBS and 0.02% sodium azide and kept at 4°C.

For immunofluorescence analysis and oil red staining after cryoprotection, liver specimens were frozen in optimal cutting temperature compound (BioOptica, Milan, Italy), and 14-μm slices were obtained in a cryostat. For Ugt1a1 immunofluorescence, liver specimens (14 μm) were incubated in sodium citrate (pH 9) prior to blocking solution. Next, specimens were blocked in 10% normal goat serum (Dako) and then incubated with the primary antibody (1:200; Sigma, St. Louis, MO) for 2 h at room temperature. Specimens were incubated with secondary antibody (Alexa fluor 488, Invitrogen). Nuclei were visualized by adding Hoechst (10 μg/mL) and mounted with Mowiol 4-88 (Sigma). Oil red staining was performed according to the manufacturer's instructions (Bioptica, Milan, Italy). Periodic-acid staining (Sigma, St. Louis, MO) was performed according to the manufacturer's instructions. For Sirius red staining, sections were de-waxed and hydrated; nuclei were stained with Weigert hematoxylin, washed in tap water, and then incubated with picro-sirius red for 1 h (Sigma, St. Louis, MO). After two washes in acidified water,

Genzyme Ex. 2020
Sarepta Therapeutics, Inc. v. Genzyme Corporation
Page 16 of 18

sections were dehydrated in absolute ethanol, cleared in xylene, and mounted in Eukitt (Sigma, St. Louis, MO). Images were acquired on a Nikon Eclipse18 E-800 epi-fluorescent microscope with a charge-coupled device camera (DMX 1200F; Nikon, 19 Amstelveen, the Netherlands). Digital images were collected using ACT-1 (Nikon) software.

Statistical Analyses

Results are expressed as mean ± SEM or mean ± SD as described in the text. The Prism package (GraphPad, La Jolla, CA) or StatistiXL plugin for windows Excel was used to analyze data and prepare the graphs. Statistical analyses have been performed by one-way or two-way ANOVA as described in the text. Values of $p < 0.05$ were considered as statistically significant.

SUPPLEMENTAL INFORMATION

Supplemental Information includes one table and seven figures and can be found with this article online at https://doi.org/10.1016/j.omtm.2018.12.011.

AUTHOR CONTRIBUTIONS

C.L.B., P.J.B., A.F.M., G.R., M.H., and F.M. contributed to the experimental design, supervised experiments and results interpretation, and wrote the manuscript. F.C., G.B., and L.G. contributed to experimental design, performed experiments and analyzed the data, and contributed to results interpretation and manuscript preparation. T.B. contributed to the GLP studies management. S.C. and L.v.W. contributed to the *in vivo* experiments. S.J.A., P. Vidal, P. Veron, M.S.S., S.R., D.G.D., F.L., C.L., and S.M. contributed to the experimental activities.

CONFLICTS OF INTEREST

F.C., G.B., G.R., P.J.B., A.F.M., and F.M. are inventors in patents describing the AAV technology and gene therapy-based treatments for Crigler-Najjar syndrome. All other authors declare no conflicts of interest with the work presented here.

ACKNOWLEDGMENTS

This work was supported by the European Union's H2020 research and innovation program under grant agreement 755225 (CureCN, coordinated by F.M.). It was also supported by Genethon, the Association Française contre les Myopathies (AFM), a grant from the CIAMI Association of Crigler-Najjar patients Italy (to F.M.), the ASTRE grant from Conseil Départemental de l'Essonne (to F.M.), a ZonMW TGO grant (to P.J.B.), the Najjar Fund (to P.J.B.), the Beneficentia Stiftung (to A.F.M.), and the EU Marie Slodowska-Curie fellowship agreement number 658712-3 (to G.R.).

REFERENCES

1. Crigler, J.F., Jr., and Najjar, V.A. (1952). Congenital familial nonhemolytic jaundice with kernicterus. Pediatrics *10*, 169–180.
2. Arias, I.M., Gartner, L.M., Cohen, M., Ezzer, J.B., and Levi, A.J. (1969). Chronic nonhemolytic unconjugated hyperbilirubinemia with glucuronyl transferase deficiency. Clinical, biochemical, pharmacologic and genetic evidence for heterogeneity. Am. J. Med. *47*, 395–409.
3. Tu, Z.H., Shang, D.S., Jiang, J.C., Zhang, W., Zhang, M., Wang, W.L., Lou, H.Y., and Zheng, S.S. (2012). Liver transplantation in Crigler-Najjar syndrome type I disease. HBPD INT *11*, 545–548.
4. Lysy, P.A., Najimi, M., Stephenne, X., Bourgois, A., Smets, F., and Sokal, E.M. (2008). Liver cell transplantation for Crigler-Najjar syndrome type I: update and perspectives. World J. Gastroenterol. *14*, 3464–3470.
5. Hafkamp, A.M., Nelisse-Haak, R., Sinaasappel, M., Oude Elferink, R.P., and Verkade, H.J. (2007). Orlistat treatment of unconjugated hyperbilirubinemia in Crigler-Najjar disease: a randomized controlled trial. Pediatr. Res. *62*, 725–730.
6. van der Veere, C.N., Sinaasappel, M., McDonagh, A.F., Rosenthal, P., Labrune, P., Odièvre, M., Fevery, J., Otte, J.B., McClean, P., Bürk, G., et al. (1996). Current therapy for Crigler-Najjar syndrome type 1: report of a world registry. Hepatology *24*, 311–315.
7. Fagiuoli, S., Daina, E., D'Antiga, L., Colledan, M., and Remuzzi, G. (2013). Monogenic diseases that can be cured by liver transplantation. J. Hepatol. *59*, 595–612.
8. Junge, N., Mingozzi, F., Ott, M., and Baumann, U. (2015). Adeno-associated virus vector-based gene therapy for monogenetic metabolic diseases of the liver. J. Pediatr. Gastroenterol. Nutr. *60*, 433–440.
9. Bortolussi, G., and Muro, A.F. (2018). Advances in understanding disease mechanisms and potential treatments for Crigler–Najjar syndrome. Expert Opin. Orphan Drugs *6*, 425–439.
10. Mingozzi, F., and High, K.A. (2011). Therapeutic in vivo gene transfer for genetic disease using AAV: progress and challenges. Nat. Rev. Genet. *12*, 341–355.
11. Nathwani, A.C., Tuddenham, E.G., Rangarajan, S., Rosales, C., McIntosh, J., Linch, D.C., Chowdary, P., Riddell, A., Pie, A.J., Harrington, C., et al. (2011). Adenovirus-associated virus vector-mediated gene transfer in hemophilia B. N. Engl. J. Med. *365*, 2357–2365.
12. Nathwani, A.C., Reiss, U.M., Tuddenham, E.G., Rosales, C., Chowdary, P., McIntosh, J., Della Peruta, M., Lheriteau, E., Patel, N., Raj, D., et al. (2014). Long-term safety and efficacy of factor IX gene therapy in hemophilia B. N. Engl. J. Med. *371*, 1994–2004.
13. George, L.A., Sullivan, S.K., Giermasz, A., Rasko, J.E.J., Samelson-Jones, B.J., Ducore, J., Cuker, A., Sullivan, L.M., Majumdar, S., Teitel, J., et al. (2017). Hemophilia B Gene Therapy with a High-Specific-Activity Factor IX Variant. N. Engl. J. Med. *377*, 2215–2227.
14. Rangarajan, S., Walsh, L., Lester, W., Perry, D., Madan, B., Laffan, M., Yu, H., Vettermann, C., Pierce, G.F., Wong, W.Y., and Pasi, K.J. (2017). AAV5-Factor VIII Gene Transfer in Severe Hemophilia A. N. Engl. J. Med. *377*, 2519–2530.
15. Miesbach, W., Meijer, K., Coppens, M., Kampmann, P., Klamroth, R., Schutgens, R., Tangelder, M., Castaman, G., Schwäble, J., Bonig, H., et al. (2018). Gene therapy with adeno-associated virus vector 5-human factor IX in adults with hemophilia B. Blood *131*, 1022–1031.
16. Bortolussi, G., Zentilin, L., Baj, G., Giraudi, P., Bellarosa, C., Giacca, M., Tiribelli, C., and Muro, A.F. (2012). Rescue of bilirubin-induced neonatal lethality in a mouse model of Crigler-Najjar syndrome type I by AAV9-mediated gene transfer. FASEB J. *26*, 1052–1063.
17. Bortolussi, G., Zentillin, L., Vaníkova, J., Bockor, L., Bellarosa, C., Mancarella, A., Vianello, E., Tiribelli, C., Giacca, M., Vitek, L., and Muro, A.F. (2014). Life-long correction of hyperbilirubinemia with a neonatal liver-specific AAV-mediated gene transfer in a lethal mouse model of Crigler-Najjar Syndrome. Hum. Gene Ther. *25*, 844–855.
18. Seppen, J., Bakker, C., de Jong, B., Kunne, C., van den Oever, K., Vandenberghe, K., de Waart, R., Twisk, J., and Bosma, P. (2006). Adeno-associated virus vector serotypes mediate sustained correction of bilirubin UDP glucuronosyltransferase deficiency in rats. Mol. Ther. *13*, 1085–1092.
19. Ronzitti, G., Bortolussi, G., van Dijk, R., Collaud, F., Charles, S., Leborgne, C., Vidal, P., Martin, S., Gjata, B., Sola, M.S., et al. (2016). A translationally optimized AAV-UGT1A1 vector drives safe and long-lasting correction of Crigler-Najjar syndrome. Mol. Ther. Methods Clin. Dev. *3*, 16049.

Genzyme Ex. 2020
Sarepta Therapeutics, Inc. v. Genzyme Corporation
Page 17 of 18

20. Bočkor, L., Bortolussi, G., Iaconcig, A., Chiaruttini, G., Tiribelli, C., Giacca, M., Benvenuti, F., Zentilin, L., and Muro, A.F. (2017). Repeated AAV-mediated gene transfer by serotype switching enables long-lasting therapeutic levels of hUgt1a1 enzyme in a mouse model of Crigler-Najjar Syndrome Type I. Gene Ther. *24*, 649–660.

21. GBD 2015 HIV Collaborators (2016). Estimates of global, regional, and national incidence, prevalence, and mortality of HIV, 1980-2015: the Global Burden of Disease Study 2015. Lancet HIV *3*, e361–e387.

22. Ayuso, E., Mingozzi, F., and Bosch, F. (2010). Production, purification and characterization of adeno-associated vectors. Curr. Gene Ther. *10*, 423–436.

23. Nathwani, A.C., Gray, J.T., Ng, C.Y., Zhou, J., Spence, Y., Waddington, S.N., Tuddenham, E.G., Kemball-Cook, G., McIntosh, J., Boon-Spijker, M., et al. (2006). Self-complementary adeno-associated virus vectors containing a novel liver-specific human factor IX expression cassette enable highly efficient transduction of murine and nonhuman primate liver. Blood *107*, 2653–2661.

24. Gunn, C.K. (1944). Hereditary Acholuric Jaundice in the Rat. Can. Med. Assoc. J. *50*, 230–237.

25. Cornelius, C.E., and Arias, I.M. (1972). Animal model of human disease. Crigler-Najjar Syndrome. Animal model: hereditary nonhemolytic unconjugated hyperbilirubinemia in Gunn rats. Am. J. Pathol. *69*, 369–372.

26. Sato, H., Aono, S., Kashiwamata, S., and Koiwai, O. (1991). Genetic defect of bilirubin UDP-glucuronosyltransferase in the hyperbilirubinemic Gunn rat. Biochem. Biophys. Res. Commun. *177*, 1161–1164.

27. Davidoff, A.M., Ng, C.Y., Zhou, J., Spence, Y., and Nathwani, A.C. (2003). Sex significantly influences transduction of murine liver by recombinant adeno-associated viral vectors through an androgen-dependent pathway. Blood *102*, 480–488.

28. McCarty, D.M., Monahan, P.E., and Samulski, R.J. (2001). Self-complementary recombinant adeno-associated virus (scAAV) vectors promote efficient transduction independently of DNA synthesis. Gene Ther. *8*, 1248–1254.

29. Manno, C.S., Pierce, G.F., Arruda, V.R., Glader, B., Ragni, M., Rasko, J.J., Ozelo, M.C., Hoots, K., Blatt, P., Konkle, B., et al. (2006). Successful transduction of liver in hemophilia by AAV-Factor IX and limitations imposed by the host immune response. Nat. Med. *12*, 342–347.

30. D'Avola, D., López-Franco, E., Sangro, B., Pañeda, A., Grossios, N., Gil-Farina, I., Benito, A., Twisk, J., Paz, M., Ruiz, J., et al. (2016). Phase I open label liver-directed gene therapy clinical trial for acute intermittent porphyria. J. Hepatol. *65*, 776–783.

31. Martino, A.T., Suzuki, M., Markusic, D.M., Zolotukhin, I., Ryals, R.C., Moghimi, B., Ertl, H.C., Muruve, D.A., Lee, B., and Herzog, R.W. (2011). The genome of self-complementary adeno-associated viral vectors increases Toll-like receptor 9-dependent innate immune responses in the liver. Blood *117*, 6459–6468.

32. Chahal, P.S., Schulze, E., Tran, R., Montes, J., and Kamen, A.A. (2014). Production of adeno-associated virus (AAV) serotypes by transient transfection of HEK293 cell suspension cultures for gene delivery. J. Virol. Methods *196*, 163–173.

33. Wright, J.F. (2014). AAV empty capsids: for better or for worse? Mol. Ther. *22*, 1–2.

34. Mingozzi, F., Anguela, X.M., Pavani, G., Chen, Y., Davidson, R.J., Hui, D.J., Yazicioglu, M., Elkouby, L., Hinderer, C.J., Faella, A., et al. (2013). Overcoming preexisting humoral immunity to AAV using capsid decoys. Sci. Transl. Med. *5*, 194ra92.

35. Nass, S.A., Mattingly, M.A., Woodcock, D.A., Burnham, B.L., Ardinger, J.A., Osmond, S.E., Frederick, A.M., Scaria, A., Cheng, S.H., and O'Riordan, C.R. (2017). Universal Method for the Purification of Recombinant AAV Vectors of Differing Serotypes. Mol. Ther. Methods Clin. Dev. *9*, 33–46.

36. Burnham, B., Nass, S., Kong, E., Mattingly, M., Woodcock, D., Song, A., Wadsworth, S., Cheng, S.H., Scaria, A., and O'Riordan, C.R. (2015). Analytical Ultracentrifugation as an Approach to Characterize Recombinant Adeno-Associated Viral Vectors. Hum. Gene Ther. Methods *26*, 228–242.

37. Favaro, P., Downey, H.D., Zhou, J.S., Wright, J.F., Hauck, B., Mingozzi, F., High, K.A., and Arruda, V.R. (2009). Host and vector-dependent effects on the risk of germline transmission of AAV vectors. Mol. Ther. *17*, 1022–1030.

38. Pañeda, A., Vanrell, L., Mauleon, I., Crettaz, J.S., Berraondo, P., Timmermans, E.J., Beattie, S.G., Twisk, J., van Deventer, S., Prieto, J., et al. (2009). Effect of adeno-associated virus serotype and genomic structure on liver transduction and biodistribution in mice of both genders. Hum. Gene Ther. *20*, 908–917.

39. Davidoff, A.M., Gray, J.T., Ng, C.Y., Zhang, Y., Zhou, J., Spence, Y., Bakar, Y., and Nathwani, A.C. (2005). Comparison of the ability of adeno-associated viral vectors pseudotyped with serotype 2, 5, and 8 capsid proteins to mediate efficient transduction of the liver in murine and nonhuman primate models. Mol. Ther. *11*, 875–888.

40. Mendell, J.R., Al-Zaidy, S., Shell, R., Arnold, W.D., Rodino-Klapac, L.R., Prior, T.W., Lowes, L., Alfano, L., Berry, K., Church, K., et al. (2017). Single-Dose Gene-Replacement Therapy for Spinal Muscular Atrophy. N. Engl. J. Med. *377*, 1713–1722.

41. Mingozzi, F., Hasbrouck, N.C., Basner-Tschakarjan, E., Edmonson, S.A., Hui, D.J., Sabatino, D.E., Zhou, S., Wright, J.F., Jiang, H., Pierce, G.F., et al. (2007). Modulation of tolerance to the transgene product in a nonhuman primate model of AAV-mediated gene transfer to liver. Blood *110*, 2334–2341.

42. Montenegro-Miranda, P.S., ten Bloemendaal, L., Kunne, C., de Waart, D.R., and Bosma, P.J. (2011). Mycophenolate mofetil impairs transduction of single-stranded adeno-associated viral vectors. Hum. Gene Ther. *22*, 605–612.

43. Snyder, R.O., Spratt, S.K., Lagarde, C., Bohl, D., Kaspar, B., Sloan, B., Cohen, L.K., and Danos, O. (1997). Efficient and stable adeno-associated virus-mediated transduction in the skeletal muscle of adult immunocompetent mice. Hum. Gene Ther. *8*, 1891–1900.

44. Thummel, C., Tjian, R., and Grodzicker, T. (1982). Construction of adenovirus expression vectors by site-directed in vivo recombination. J. Mol. Appl. Genet. *1*, 435–446.

45. Meliani, A., Boisgerault, F., Fitzpatrick, Z., Marmier, S., Leborgne, C., Collaud, F., Simon Sola, M., Charles, S., Ronzitti, G., Vignaud, A., et al. (2017). Enhanced liver gene transfer and evasion of preexisting humoral immunity with exosome-enveloped AAV vectors. Blood Adv. *1*, 2019–2031.

46. Montenegro-Miranda, P.S., Pañeda, A., ten Bloemendaal, L., Duijst, S., de Waart, D.R., Gonzalez- Aseguinolaza, G., and Bosma, P.J. (2013). Adeno-associated viral vector serotype 5 poorly transduces liver in rat models. PLoS ONE *8*, e82597.

Genzyme Ex. 2020
Sarepta Therapeutics, Inc. v. Genzyme Corporation
Page 18 of 18